EFFECT OF WEATHERING ON MECHANICAL DEGRADATION OF SANDSTONES

Pratabjai Prasujan

A Thesis Submitted in Partial Fulfillment of the Requirements for the Degree of Master of Engineering in Civil, Transportation and Geo-Resources Engineering

Suranaree University of Technology

Academic Year 2020

ผลกระทบของการผุกร่อนต่อการเสื่อมเชิงกลของหินทราย

นางสาวประทับใจ พระสุจันทร์

วิทยานิพนธ์นี้เป็นส่วนหนึ่งของการศึกษาตามหลักสูตรปริญญาวิศวกรรมศาสตรมหาบัณฑิต
สาขาวิชาวิศวกรรมโยธา ขนส่ง และทรัพยากรธรณี
มหาวิทยาลัยเทคโนโลยีสุรนารี
ปีการศึกษา 2563

EFFET OF WEATHERING ON MECHANICAL DEGRADATION OF SANDSTONES

Suranaree University of Technology has approved this thesis submitted in partial fulfillment of the requirements for a Master's Degree.

Thesis Examining Committee

(Assoc. Prof. Dr. Pornkasem Jongpradist)

Chairperson

(Prof. Dr. Kittitep Fuenkajorn)

Member (Thesis Advisor)

(Asst. Prof. Dr. Akkhapun Wannakomol)

Member

(Dr. Thanittha Thongprapha)

Member

(Assoc. Prof. Flt. Lt. Dr. Kontorn Chamniprasart)

Vice Rector for Academic Affairs

and Internationalization

(Assoc. Prof. Dr. Pornsiri Jongkol)

Dean of Institute of Engineering

ประทับใจ พระสุจันทร์ : ผลกระทบของการผุกร่อนต่อการเสื่อมเชิงกลของหินทราย (EFFECT OF WEATHERING ON MECHANICAL DEGRADATION OF SANDSTONES) อาจารย์ที่ปรึกษา : ศาตราจารย์ ดร. กิตติเทพ เฟื่องขจร, 75 หน้า

การจำลองการผุกร่อนได้ดำเนินการบนหินทรายจำนวน 4 ชนิด โดยทดสอบภายใต้วัฏจักรร้อน-เย็น มากถึง 300 รอบ หินทรายแต่ละชนิดได้ถูกทดสอบภายใต้ 3 สภาวะ คือ การปล่อยให้เย็นที่อุณหภูมิห้อง การจุ่มลงในน้ำกลั่น และการจุ่มลงในกรดซัลฟิวริก (ค่าความเป็นกรดเท่ากับ 5.6) ผลที่ได้ระบุว่าหินทรายทุกชนิดไม่อ่อนไหวต่อวัฏจักรร้อน-เย็นแบบแห้ง อย่างไรก็ตาม หินทรายเหล่านี้อ่อนไหวอย่างมากต่อน้ำและกรด การลดอุณหภูมิอย่างฉับพลันของหินที่จุ่มลงในของเหลวทำให้เกิดรอยแตกขนาดเล็กในวัสดุเชื่อมประสาน ซึ่งต่อมาได้กลายเป็นช่องเปิดให้ของเหลวซึมลึกลงไปในตัวอย่างหิน เมื่อวัสดุเชื่อมประสานถูกละลายด้วยของเหลว ส่งผลให้ความหนาแน่น ความแข็ง และความเหนียวของหินทรายมีค่าลดลงเมื่อจำนวนรอบวัฏจักรการจำลองเพิ่มขึ้น อัตราส่วนปัวส์ซองมีค่าเพิ่มขึ้นตามจำนวนรอบของวัฏจักรเนื่องจากการเพิ่มขึ้นของความพรุนของหิน การค้นพบนี้จะเป็นประโยชน์สำหรับการเลือกสรรและการประยุกต์ใช้ของหินทรายเหล่านี้ในอุตสาหกรรมหินก่อสร้างและหินประดับ

สาขาวิชา เทคโนโลยีธรณี

ปีการศึกษา 2563

ลายมือชื่อนักศึกษา ประทับใจ

ลายมือชื่ออาจารย์ที่ปรึกษา K. Fuenkajorn

PRATABJAI PRASUJAN : EFFECT OF WEATHERING ON MECHANICAL DEGRADATION OF SANDSTONES. THESIS ADVISOR : PROF. KITTITEP FUENKAJORN, Ph.D., P.E. 75 PP.

STRENGTH/ ELASTIC MODULUS/ DENSITY/ POROSITY

Weathering simulations have been performed on four sandstone types by subjecting them up to 300 heating-cooling cycles. Three cooling conditions are imposed on three separate sets of specimens prepared from each sandstone type: air-cooling, submerging in distilled water and in sulfuric acid (pH = 5.6). Results indicate that all sandstones are insensitive to heating-dry cooling cycles. They are however highly sensitive to water and particularly to acid. Such rapid cooling in liquid induces micro-cracks in the cementing materials, which become preferential paths allowing liquid to penetrate deeper into the specimens. As the cementing materials are dissolved by the liquids, the sandstone density, strength and stiffness decrease as the simulation cycles increase. Poisson's ratio increases with the test cycles due to increase of rock porosity. The findings can be useful for the selection criteria and application of these sandstones in the construction and decoration industry.

School of Geotechnology　　　　Student's Signature ______________

Academic Year 2020　　　　Advisor's Signature ______________

ACKNOWLEDGMENTS

I wish to acknowledge the funding supported by Suranaree University of Technology (SUT).

I would like to express my sincere appreciation to Professor Dr. Kittitep Fuenkajorn for his valuable guidance and efficient supervision. I appreciate his encouragement, strong support, comments, and suggestions throughout the research period. I also would like to express my gratitude to Dr.Thanitha Thongprapha for comment and support on my research works, Associate Professor Dr.Anisong Chitnarin, Miss Laksikar Sitthimongkol and Mister Pittawat Liapkrathok for their laboratory advice, ,Komsun Taisup and Yuthika Sroiraya for X-ray diffraction analysis advice. Grateful thanks are given to all staffs of Geomechanics Research Unit, Institute of Engineering who supported my work.

Finally, I would like to thank beloved parents for their love, support, and encouragement.

Pratabjai Prasujan

TABLE OF CONTENTS

Page

TABLE OF CONTENTS (Continued)

Page

TABLE OF CONTENTS (Continued)

Page

LIST OF TABLES

LIST OF TABLES (Continued)

Table **Page**

LIST OF FIGURES

Figure **Page**

LIST OF FIGURES (Continued)

Figure **Page**

LIST OF FIGURES (Continued)

Figure **Page**

LIST OF FIGURES (Continued)

Figure **Page**

SYMBOLS AND ABBREVIATIONS

α	=	Empirical constant
β	=	Empirical constant
ε_{axial}	=	Axial strain
ε_{lat}	=	Lateral strain
ν	=	Poisson's ratio
$\nu_{(N)}$	=	Poisson's ratio
σ_1	=	Uniaxial compressive strength
σ_c	=	Uniaxial compressive strength
$\sigma_{c,(N)}$	=	Uniaxial compressive strength at various number of test cycles
σ_t	=	Tensile strength
$\sigma_{t,(N)}$	=	Tensile strength at various number of test cycles
A	=	Mass of over-dry test sample in air
B	=	Mass of test sample in air
b	=	Specimen width
C	=	Apparent mass of test sample in water
d	=	Specimen thickness
E_c	=	Compressive elastic modulus
$E_{c,(N)}$	=	Compressive elastic modulus at various number of test cycles
E_t	=	Tensile elastic modulus
$E_{t,(N)}$	=	Tensile elastic modulus at various number of test cycles
L	=	Support span length

SYMBOLS AND ABBREVIATIONS (Continued)

N	=	Number of test cycles
P	=	Maximum applied load
Q_e	=	Equivalent quartz content
SG	=	Specific gravity
$SG_{(N)}$	=	Specific gravity at various number of test cycles

CHAPTER I

INTRODUCTION

1.1 Background and Rationale

Sandstone, a common sedimentary rock, is widely distributed on the earth surface. It is also a material used in heritage buildings due to the high degree of cementation as a calcareous or siliceous material and its local availability (Sun and Zhang, 2019). Hence, many buildings and monuments have used sandstones. These include, for examples, the Schloss Johannisburg (a château) in Germany (Siedel et al., 2003), the Corbii de Piatra church in Romania (Barzoi and Luca, 2013), the Museum of Contemporary Art in Sydney (Franklin et al., 2014), the San Gimignano towers with Tuscany architecture in Italy (Andreotti et al., 2018) and the Angkor temples in Cambodia (Xu et al., 2018). Seasonal changes in groundwater level and humidity can lead to cyclic actions of wetting and drying and accelerate the weathering process of the rocks, which over the years would eventually result in deterioration and even damage (Zhou et al., 2017).

Even though, the influence of weathering processes on the physical and mechanical properties of rock has been studied by many researchers, an attempt at investigating the long-term durability of rocks has rarely been addressed. The rock deterioration after weathering processes under wetting and drying cycles was assessed by changes in physical properties including bulk density, weight loss, water absorption (water content), effective porosity, P-wave velocity, etc. (Pardini et al., 1996; Sumner and Loubser, 2008; Özbek, 2014; Khanlari and Abdilor, 2015). This relatively short-term testing may not be sufficient to distinguish some rocks with similar strength and compositions, and in particularly to determine their long-term durability under different environmental conditions.

1.2 Research Objectives

The objective of this study is to simulate the effect of weathering on the physical, mechanical and mineralogical properties of four sandstones commonly used in construction and decorating industry in southeast Asia. The simulation is made under 300 heating and cooling cycles. Three separate sets of specimens are cooled under three different conditions: dry, wet and acidic conditions. For every 100 cycles, the physical, mechanical and mineralogical properties of the specimens are determined.

1.3 Scope and Limitations

The scope and limitations of this study include as follows:

1) Four sandstone types are prepared: Phu Phan sandstone, Phu Kradung sandstone, Sao Khua sandstone and Phra Wihan sandstone.

2) Simulation of rock degradation are performed under thermal, dry, wet and acidic conditions up to 300 cycles.

3) For testing under acidic condition, an acid solution with pH=5.6 is used from concentrated sulfuric acid mixed with distilled water.

4) The testing to investigate the physical (specific gravity) and mechanical (tensile strength, tensile elastic modulus, compressive strength, compressive elastic modulus and Poisson's ration) properties are performed for every 100 cycles.

5) Specific gravity test follows the ASTM C127-15 standard practice.

6) Three-point bending test procedure and calculation follow the ASTM C293/C293M-16 standard practices.

7) Uniaxial compressive strength test is conducted following ASTM D7012-14e1 standard practice.

8) Mineral compositions are determined by using X-ray diffraction following the ASTM STP 479 standard practice.

9) The research findings are published in conference paper and journal

1.4 Research Methodology

The research methodology (Figure 1.1) comprises 9 steps; including literature review, sample collection and preparation, laboratory simulation of rock degradation, water absorption test, three-point bending test, uniaxial compressive strength test, X-ray diffraction, result analysis, discussions, conclusions and thesis writing.

1.4.1 Literature review

Literature review is carried out to study about weathering process and effect of degradation on rock properties. The sources of information are from journals, technical reports and conference papers. A summary of the literature review is given in the thesis.

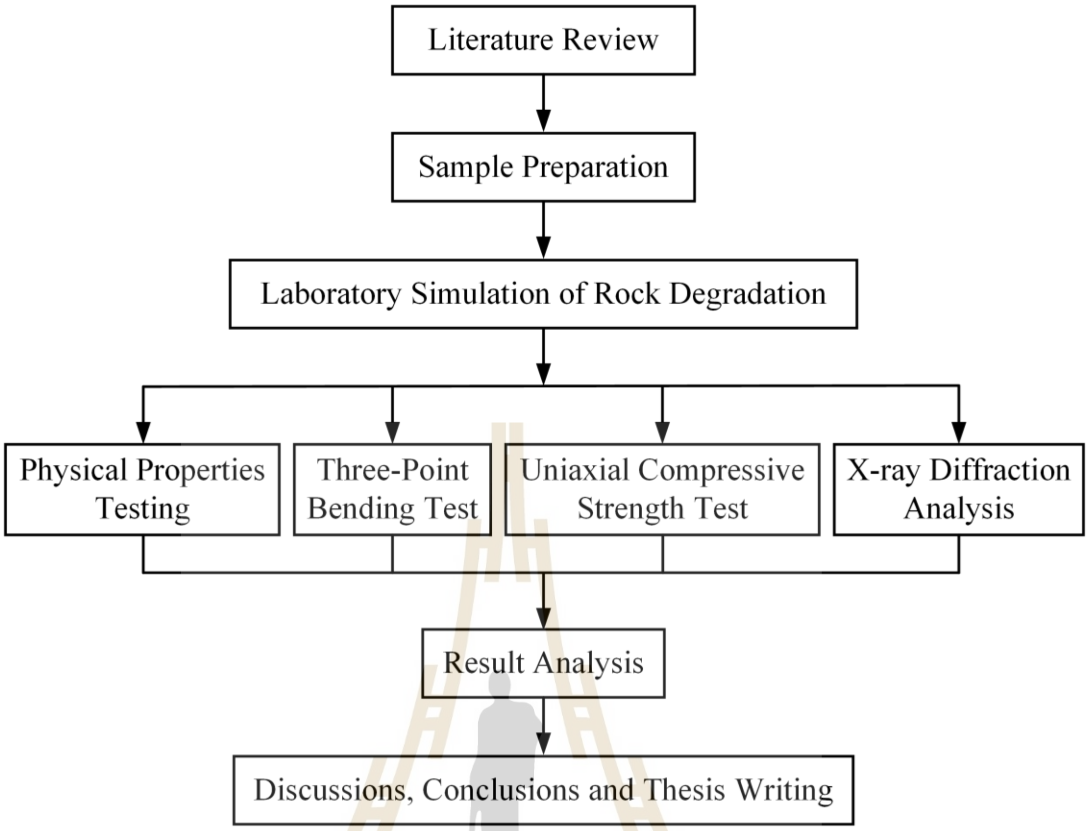

Figure 1.1 Research methodology.

1.4.2 Sample preparation

The rock samples used in this study are collected from the Khorat group including Phu Kradung sandstone, Phra Wihan sandstone, Sao Khua sandstone and Phu Phan sandstones. The collected sandstone blocks are cut and ground to obtain prismatic specimens with nominal dimensions of 35×35×152 mm^3. Twenty specimens are prepared for each sandstone type.

1.4.3 Laboratory Simulation of degradation

The simulation of rock degradation is investigated under dry, wet and acidic conditions of cyclic process. A total of 300 cycles is carried out for each rock type specimen. The specific experimental details are listed as follows:

1) Dry condition; Testing under ambient temperature (25±2 °C) for 12 hrs, and then put in the sample dry oven (105±5 °C) for 12 hrs (per 1 cycle).

2) Wet condition; Submerge in water for 12 hrs, and then put in the sample dry oven (105±5 °C) for 12 hrs (per 1 cycle).

3) Acidic condition; Submerged in sulfuric acid for 12 hrs, and then put in the sample dry oven (105±5 °C) for 12 hrs (per 1 cycle).

1.4.4 Physical properties testing

Physical properties tests (ASTM C127-15) is performed to determine the apparent specific gravity, and absorption of the rock specimens under various stages of weathering. The samples will be investigated at initial and after every 100 cycles (for a total of 300 cycles) of simulation on rock degradation. The result will be presented in term of the absorbed rate of rock specimen under various environmental conditions.

1.4.5 Three-point bending test

Three-point bending test following ASTM C293/C293M-16 standard practice will be performed to determine the effect of rock degradation on tensile strength and tensile modulus of sandstones. Figure 5 shows the positions of the loading for the upper and lower bearing plates. A data logger (TC-32K) connected with the switching box (Type B-2760) will be used to monitor the induced tensile strains. The testing will be conducted at initial and after every 100 cycles (for a total of 300 cycles).

1.4.6 Uniaxial compressive strength test

The uniaxial compressive strength test method and calculation follow the ASTM D7012-14e1 standard practice. The testing will be performed by increasing the axial stress to the rock specimen. The dial gages will be installed to measure the axial and lateral strains. During the test, the axial strain and lateral strain will be monitored. The results will be used to determine the compressive strength, elastic modulus and Poisson's ratio and revealing the effect of rock degradation at initial and after every cycle of thermal, drying, wetting, and acidic conditions.

1.4.7 X-ray diffraction (XRD) analysis

The XRD analysis is performed on finely ground rock powder pressed into coherent pellets. The analysis will be performed at initial and after every 100 cycles (for a total of 300 cycles) of simulation on rock degradation. The result can be used to identify the effect of rock degradation on changing to mineral compositions which may affect rock stability.

1.4.8 Result analysis

The results obtained from the three-point bending test, uniaxial compressive strength test and XRD analyses after simulation on rock degradation is compared and analyzed to determine the mathematical relationship equations for use to predict the long-term stability of the four sandstones.

1.4.9 Discussions, conclusions and thesis writing

Discussions will be made on the reliability and adequacies of the approaches used here. Future research needs are identified. All research activities, methods, and results will be documented and complied in the thesis. The research or findings are published in the conference proceedings and journals.

1.5 Thesis content

This research thesis is divided into seven chapter. The first chapter includes background and rational, research objectives, scope and limitations and research methodology. Chapter two present summary result of literature review to improve an understanding of the effect of weathering on mechanical degradation of rock. Chapter three describes sample preparation. Chapter four describes laboratory testing and methods for rock degradation simulations. Chapter five describes the results of rock degradation simulations. Chapter six presents analysis of test result. Chapter seven presents the discussion, conclusions, and recommendations for future studies.

CHAPTER II

LITERATURE REVIEW

2.1 Introduction

This chapter summarizes of literature review will be carried out to improve an understanding weathering process of rock. The topics reviewed include the definition of weathering, chemical and mechanical weathering.

2.2 Definition of weathering

There are two types of weathering: chemical weathering due to mechanical weathering and chemical attentions as results of wind, thermal cycles, freeze-thaw cycles, and erosion by surface water. Chemical weathering is the attention of rock forming minerals by chemical agents, acid in air, in surface water and in rain. Mechanical weathering is a process by which rock is broken into small fragments as a result of energy developed by physical forces. (Abramson et al., 1995).

Yokota and Iwamatsu (1999) study the weathering process of soft pyroclastic rocks composing the many weakly interlocked volcanic glass and pumice fragments. Their physical properties depend on the degree of welding. A pyroclastic rock is generally like sandstone about its engineering properties. The weathering and softening of rocks are due to changes not only in the physical and mechanical characteristics, but also in the chemical properties of the rocks. Mechanical changes include that the surface tends to loosen easily and disintegrates at an early stage. The unlocking mechanism of volcanic glass may also be considered as a mechanical change.

The dissolution of chemical components, such as ferric oxide and silica, which serve as intergranular cement, and volcanic glass may also commence at an early stage. Although the processes involved in both mechanical disintegration and chemical dissolution are difficult to measure, they may be the dominant weathering processes in these rocks.

Moon and Jayawardane (2004) study the geochemical and geomechanical weathering of Karamu basalt in New Zealand. They concluded that the early stages of weathering as initial fracturing of the rock were physical processes, followed by the progressive development of secondary minerals that reduced the strength of the rocks. From these results, it is apparent that an early loss of alkaline earth elements (magnesium, calcium and ferrous) can be measured geochemically before any significant mineralogical change occurs and is closely linked to a dramatic drop in the intact strength of slightly weathered basalt.

2.3 Chemical weathering

2.3.1 Field study

Weathering processes cause important changes in rock porosity. Besides porosity, distribution of pore sizes is significant for the identification of changes of changes due to rock weathering and its effect on fabric (Tugrul, 2004).

In urban or highly industrialized areas, other gases of an acidic nature are produced from combustion of fuels. In the case of sulfur component, sulfur trioxide dissolves in water to produce sulfuric acid (Charola, 1987). In Thailand have the Acid Deposition Monitoring Network in East Asia (EANET) state of acid deposition in country and the national measures implemented. Resulted monitoring of environment from 2010-2014, the rain is pH about 5.6 (Lee, 2016).

Özbek., (2014) study effects of wetting-drying and freezing-thawing cycles on some physical and mechanical properties of ignimbrites (black, red, yellow, gray) from Central Anatolia. Physical and mechanical properties of each sample were determined every 10 cycles (for a total of 50 cycles). The freezing and thawing treatment caused larger changes of physical and mechanical properties than the wetting and drying treatment (Figure 2.1). The mineral compositions may be an important factor on the results. The dissolution, hydration, swelling, durability, and sensitivity to chemical degradation of each mineral determine how the mineral weathering row depends on the cycle. Soft minerals can easily decompose after few cycles, more resistant minerals may decompose during several cycles.

Torres-Suarez et al., (2014) study The techniques such as vapor equilibrium technique were used to control relative humidity (suction- controlled) and to apply wetting-drying cycles and loading-unloading cycles through ultrasonic wave velocities The main failure mechanisms for the laminated mudrocks start on the microscopic scale by fissures coalescence, exhibiting physical-chemical degradation as well. When compared with in situ conditions, the obtained results can provide engineering values according to monitoring laboratory set.

Khanlari and Abdilor, (2015) study the effects of wet–dry, heat-cool, and freeze–thaw cycles on the physical and mechanical properties of Upper Red Formation sandstones. Five different types of sandstones were selected, and wet–dry, heat–cool, and freeze–thaw cyclic tests were performed. The results also show that the presence of zeolite cement has a significantly effect on sandstone resistance to freeze–

thaw cycles. It has been found that sandstone strength as well as petrographic properties do not have significant effect on sample deterioration during freeze–thaw cycles. Finally, it was concluded that pore size plays an important role in sandstone resistance to freeze–thaw cycles.

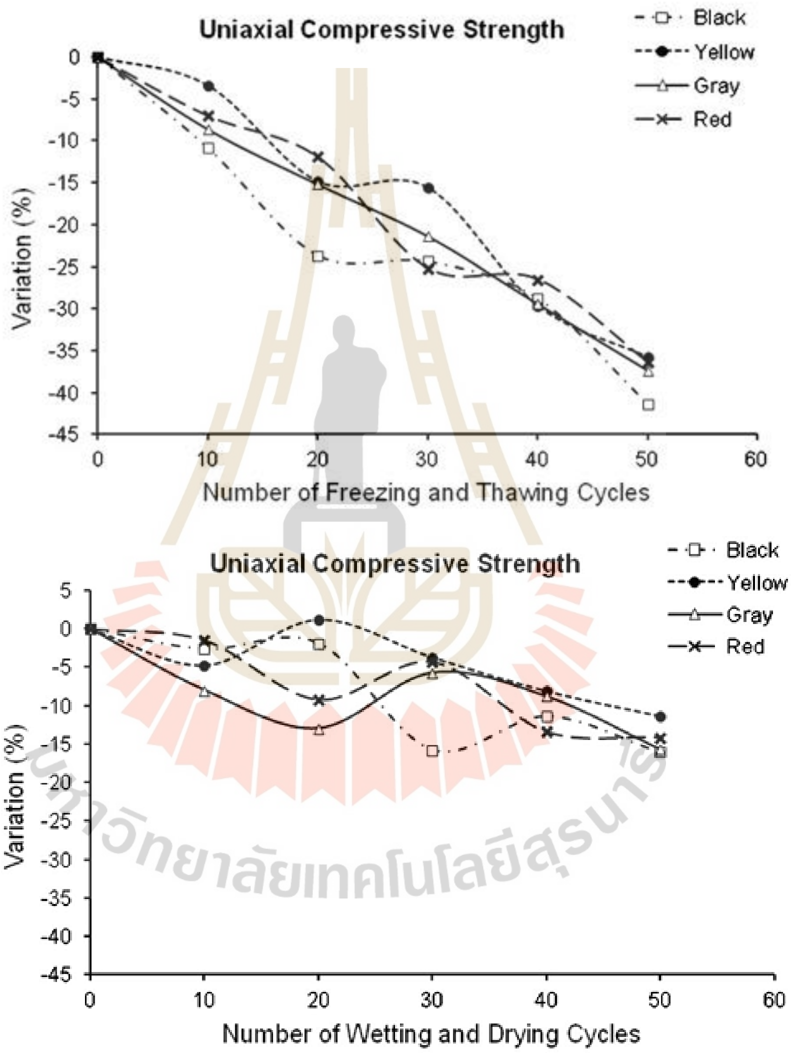

Figure 2.1 Changes in the uniaxial compressive strength values of the ignimbrite samples (Özbek, 2014).

2.3.2 Laboratory testing

The cyclic wetting-drying phenomenon plays a vitally important role in affecting the properties of rock materials. (Zhou et al., 2017). To investigate physical properties of sandstone specimens, slake durability index (SDI) and P-wave velocity are measured after every 10 cycles. They found that with the increase of wetting and drying cycles, the water absorption and porosity of rock increases while the density, SDI, and P-wave velocity decrease. The rock degradation after wetting and drying cycles are assessed by changes in physical and mechanical properties including weight loss, water absorption (water content), effective porosity, bulk density, P-wave velocity (Pardini et al., 1996; Sumner and Loubser, 2008), uniaxial compressive strength (Hale and Shakoor, 2003; Ning et al., 2003; Lin et al., 2005; Deng et al., 2012), tensile strength (Liu et al., 2016; Zhao et al., 2017), shear strength (Zhang et al., 2015) and fracture toughness (Hua et al., 2015). The physical properties of rock materials have a different degree of deterioration after drying and wetting cycles. Zhou et al., (2017) study the influence of cyclic wetting and drying on dynamic compressive properties of sandstone. Dynamic compressive tests were conducted using a modified split Hopkinson pressure bar (SHPB) technique for rock specimens. The results indicate that, with the increase of cyclic wetting and drying, dynamic compressive strength and elastic modulus decrease (Figure 2.2).

Gupta and Ahmed (2007) investigate the effect of mineralogical properties and pH of water on degradability of different rocks. The degradability of rocks is significantly affected by the texture and mineral composition. Rocks contain an appreciable amount of calcium carbonate (about 60%). Degradability is higher in acidic solution environments on carbonate rocks.

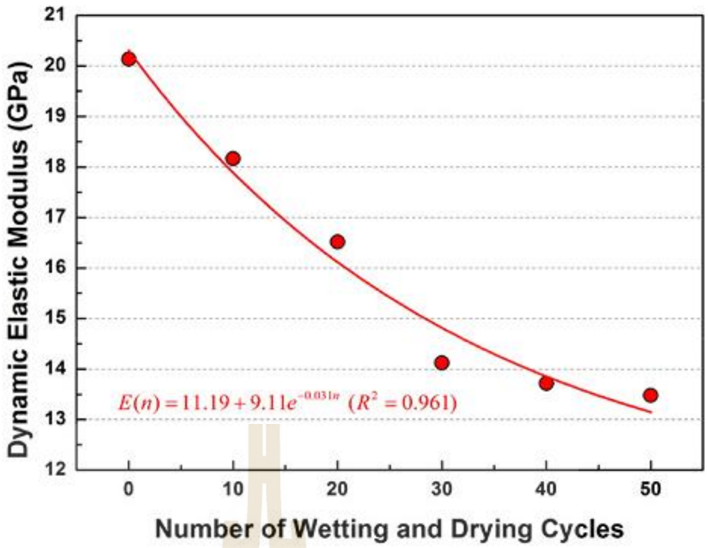

Figure 2.2 Dynamic elastic modulus of specimens at the strain rate of $90s^{-1}$ versus number of wetting and drying cycles (Zhou et al., 2017).

Ghobadi and Momeni (2011) assess the granitic rocks degradability by acid environment in urban area. The rocks posse are very high durability. Despite long-term effects such as weathering process can cause serious problems to ancient buildings as in inscription of Darius.

The resistance to weathering of rock depends on types of exposed surface area, porosity of rocks and mineral composition. Weathering is not only dependent on the mineral compositions but also on the porosity of the rock (Robinson and Williams, 1994). Rocks consisting of coarse fragments such as granite easily weather physically but do not weather chemically fast. In contrast, in rock consisting of fine fragments, such as basalt, chemical weathering is quicker than physical weathering. The weathering of stratified sedimentary rocks is dependent on the orientation of the stratification and cementation. The ranking of some primary minerals in order of increasing stability is shown in Figure 2.3 Olivine weathers rapidly because the silicon tetrahedral is only held together by oxygen and the metal cations which form weak bonds. In contrast, quartz is very resistant, because it consists entirely of linked silicon tetrahedral. The mean lifetime of one millimeter of different rocks into a kaolinitic saprolite is shown in Table 2.1. These numbers suggest that in cold or tropical humid zone, the climate controls the rate of weathering

2.4 Mechanical weathering

Gökceoğlu et al. (2000) investigate the factors affecting the slake durability index (SDI) of 17 kinds of clay-bearing rocks and emphasized the influence of the number of wetting and drying cycles on the SDI values. The results indicate that the type and amount of clay minerals are the main factors influencing the variations of the slake durability index in all samples, the slake durability index decreased with increasing number of wetting and drying cycles because the weakening of the intergranular bonds occur easier.

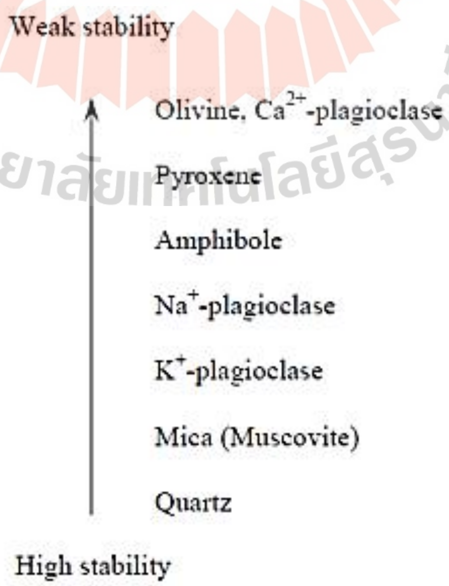

Figure 2.3 Stability of some primary minerals (Robinson and Williams, 1994).

Table 2.1 Mean lifetime of one millimeter of fresh rock (Nahon, 1991).

Rock Type	Climate	Lifetime (years)
Acid rocks	Tropical semi-arid Tropical humid Temperate humid Cold humid	65 to 200 20 to 70 41 to 250 35
Metamorphic rocks	Temperate humid	33
Basic rocks	Temperate humid Tropical humid	68 40

Sri-in and Fuenkajorn (2007) and Fuenkajorn and Sri-in (2009) experimentally assess the degrees of rock durability as it is subjected to the cyclic changes of temperature, slaking and humidity on thirteen rock types. The results show that Phra Wihan siltstone, Chonburi quartz mica schist, and Pichit pumice breccia have a higher rate of weight loss than the other rocks (Figure 2.4). Phra Wihan siltstone shows that the P-wave velocity decreases with increasing numbers of heating and cooling cycles. This is probably due to the high percentage of weight loss in rock specimen, and therefore decreasing its density. Phu Kradung sandstone, Kaeng Krachan micaceous siltstone, and Khok Kruat sandstone have a lower rate of wave velocity decrease. The increase of the apparent porosity of the rocks with increasing number of heating-cooling cycles.

Finer grained sediments are more susceptible to breakdown and at higher rates than coarse grained sedimentary materials (Andrews et al., 1980; Kolay and Kayabali, 2006). Although there are conflicting findings, fine grained samples can withstand higher uniaxial compressive loads (Brace, 1961; Fahy and Guccions, 1979). This may be because the number of grains to grain contacts is higher for fine grained samples. The applied external force is distributed over a larger contact surfaces.

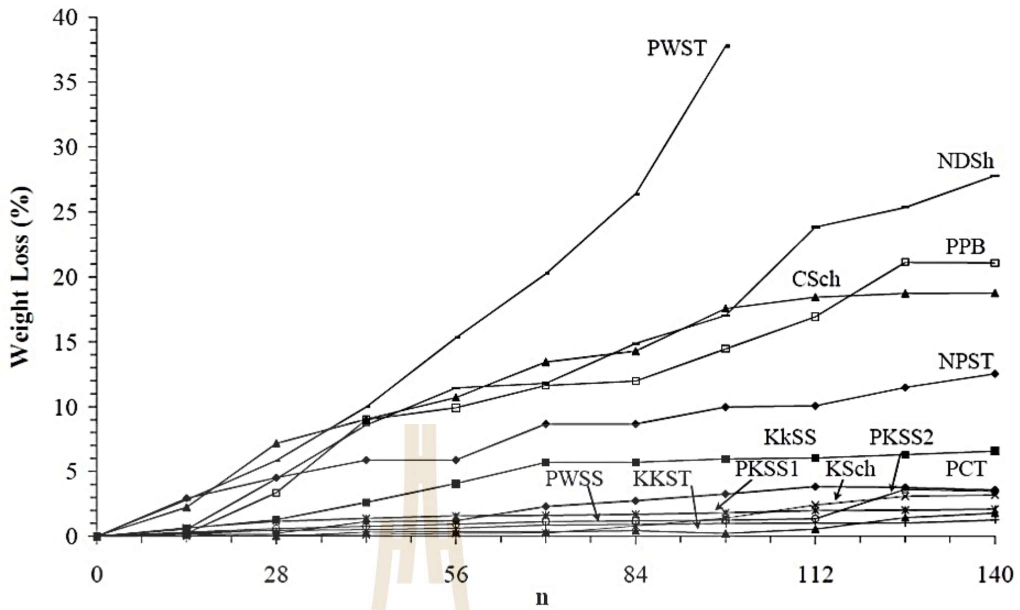

Figure 2.4 Weigh loss of rock specimens monitored every 14 cycles of heating and cooling cycles (Fuenkajorn and Sri-in, 2009).

Rocks made of rounded grains are more durable (Andrews et al., 1980) because crystals or grains with sharp edges are exposed to a greater degree of abrasion during the slake durability test, resulting in lower slake durability indices. Stresses will concentrate along grain edges in the uniaxial compression test. Depending on the degree of bonding between the grains, such angular shaped particles may provide a great deal of interlocking thus increasing the compressive strength. Several researchers (Fahy and Guccions, 1979; Ulusay et al., 1994; Shakoor and Bonelli, 1991) report positive correlation between the uniaxial compressive strength and percentage of angular grains. Assuming properties such as cement and mineralogy of grains and degree of bonding are the same, a rock made of angular grains should be stronger and harder (due to better interlocking of grains) but less durable (due to higher degree of erosion) than a rock composed of rounded grains. Type of grain contacts and grain boundaries are likely to affect the strength of rock material (Ulusay et al., 1994; Shakoor and Bonelli, 1991). These researchers found a significant positive correlation between these variables and uniaxial compressive strength of sandstone samples. Since sutured contacts provide better interlocking of grains, these types of contacts should increase the hardness and durability of specimens also.

Bell (1978) correlates packing density, which is the space occupied by grains in each area, with the uniaxial compressive and tensile strengths of Fell sandstone. The results that strength increased with increasing packing density. Hoek (1965) suggests that severe interlocking of grains could occur in sedimentary rocks in which grains have been tightly packed and well cemented. This would result in a considerable increase in the amount of applied stress required to propagate grain boundary cracks. Shakoor and Bonelli (1991) did not find any significant relationship between packing density and strength.

The mineralogy and the geometric arrangement (microfabric) of particles affect slaking and strength of weak rocks. As a rock forming mineral, most of the correlations established by previous researchers (Fahy and Guccions, 1979; Gunsallus and Kulhawy, 1984; Shakoor and Bonelli, 1991) found a negative relationship between quartz content and uniaxial compressive strength of the investigated sandstones. Handlin and Hager (1957); Bell (1978); Barbour et al. (1979); Tugrul and Zarif 1999; Yusof and Zabidi (2016) did not find any significant correlation and suggested that the structural interlocking of the quartz grains and not the quartz content itself influences uniaxial compressive strength. Also, while not clearly stated in the literature, it is believed that rocks composed of quartz grains should have a higher durability due to the higher resistance of this mineral to mechanical abrasion.

CHAPTER III

SAMPLE PREPARATION

3.1 Introduction

This chapter describes the rock sample preparation procedure for the simulation of rock degradation by three-point bending test, uniaxial compression test and X-ray diffraction analysis. Four type of Thai sandstone are used in this study.

3.2 Sample preparation

3.2.1 Simulation of degradation

Rock samples in this study belong to Phu Kradung, Phra Wihan, Sao Khua and Phu Phan sandstone formations. The collected sandstone blocks are cut and ground to obtain prismatic specimens with nominal dimensions of 35×35×152 mm^3 (Figure 3.1). Twenty specimens are prepared for each sandstone type. Tables 3.1 though 3.4 shows the dimensions of sandstone prepared for testing under initial, dry, wet and acidic conditions.

3.2.2 Three-point bending test specimens

The specimens are subjected to three-point bending test (ASTM C293-16) to determine their bending tensile strength. A strain gage is installed at the incipient crack initiation point (Figure 3.2). Its readings can provide tensile strains which can be later used to determine tensile deformation (elastic) modulus before failure occurs. Gage length used here is 10 mm and gage factor is 2.13 ± 1%.

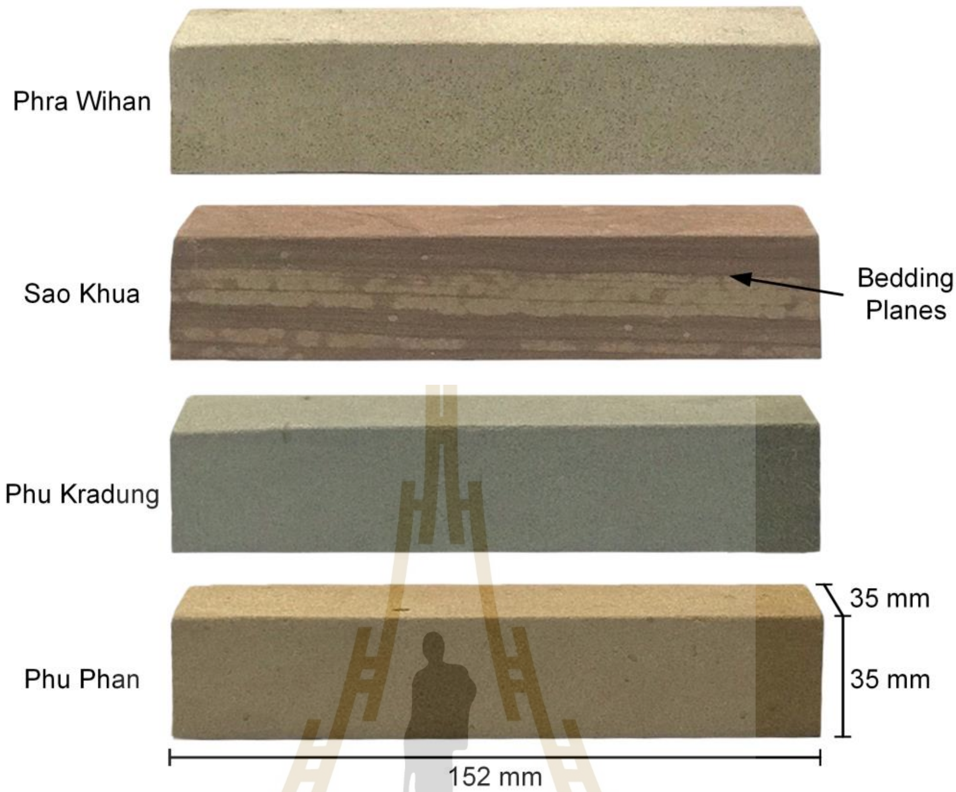

Figure 3.1 Sandstone specimens prepared for simulation of degradation.

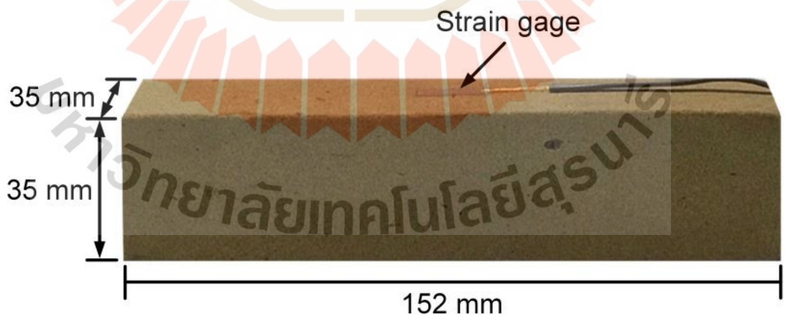

Figure 3.2 Example sandstone specimens with strain gage installed for three-point bending test.

Table 3.1 Phu Phan specimens prepared for simulation of degradation and three-point bending test.

Specimen No.	Thickness, d (mm)	Width, b (mm)	Length (mm)	Weight (g)
PP-Initial-01	33.87	34.65	151.72	405.92
PP-Initial-02	34.61	35.07	151.64	426.46
PP-100-Dry-01	34.37	35.19	151.24	424.81
PP-100-Dry-02	34.88	33.73	152.50	410.08
PP-200-Dry-01	33.73	35.47	151.40	419.51
PP-200-Dry-02	33.11	33.87	152.04	393.05
PP-300-Dry-01	33.87	34.57	152.30	409.15
PP-300-Dry-02	35.50	33.15	151.70	417.65
PP-100-Wet-01	33.79	35.26	152.00	417.84
PP-100-Wet-02	35.24	36.97	152.16	447.74
PP-200-Wet-01	36.99	34.05	151.70	442.31
PP-200-Wet-02	32.27	35.53	152.04	406.37
PP-300-Wet-01	33.30	31.35	152.00	367.37
PP-300-Wet-02	31.95	33.40	152.15	381.54
PP-100-Acid-01	32.05	33.61	152.16	379.48
PP-100-Acid-02	31.27	31.14	151.38	342.57
PP-200-Acid-01	33.45	35.85	151.95	417.53
PP-200-Acid-02	34.25	33.00	151.10	400.02
PP-300-Acid-01	35.15	36.00	151.40	444.94
PP-300-Acid-02	35.11	35.05	151.20	431.49

Table 3.2 Phu Kradung specimens prepared for simulation of degradation and three-point bending test.

Specimen No.	**Thickness, d (mm)**	**Width, b (mm)**	**Length (mm)**	**Weight (g)**
PK-Initial-01	31.70	34.95	151.90	424.94
PK-Initial-02	33.10	32.45	153.70	418.71
PK-100-Dry-01	31.50	33.15	151.70	401.52
PK-100-Dry-02	31.45	33.75	151.45	401.57
PK-200-Dry-01	33.24	33.00	151.95	418.57
PK-200-Dry-02	33.30	36.70	151.95	466.61
PK-300-Dry-01	32.60	31.95	151.30	403.17
PK-300-Dry-02	35.80	36.90	151.90	502.24
PK-100-Wet-01	33.10	31.65	153.60	408.04
PK-100-Wet-02	32.60	33.40	148.55	376.27
PK-200-Wet-01	35.90	38.65	151.70	524.73
PK-200-Wet-02	34.50	32.50	151.90	440.48
PK-300-Wet-01	32.05	30.85	148.90	345.12
PK-300-Wet-02	29.15	35.25	152.00	461.51
PK-100-Acid-01	36.35	33.40	152.25	462.93
PK-100-Acid-02	35.45	33.65	152.25	456.71
PK-200-Acid-01	34.20	33.85	151.75	445.24
PK-200-Acid-02	36.30	35.70	151.75	483.75
PK-300-Acid-01	35.35	34.40	151.85	452.71
PK-300-Acid-02	35.15	32.65	152.35	445.10

Table 3.3 Sao Khua specimens prepared for simulation of degradation and three-point bending test.

Specimen No.	Thickness, d (mm)	Width, b (mm)	Length (mm)	Weight (g)
SK-Initial-01	36.25	34.49	152.66	455.50
SK-Initial-02	35.55	34.36	151.76	439.32
SK-100-Dry-01	36.44	36.36	151.74	477.37
SK-100-Dry-02	35.15	32.65	152.00	419.19
SK-200-Dry-01	35.93	35.00	151.94	451.86
SK-200-Dry-02	32.25	38.83	152.00	453.50
SK-300-Dry-01	34.91	32.70	152.52	417.55
SK-300-Dry-02	32.29	33.61	152.66	387.71
SK-100-Wet-01	33.24	33.65	152.00	413.37
SK-100-Wet-02	34.49	32.30	151.66	394.94
SK-200-Wet-01	36.62	34.07	151.52	447.68
SK-200-Wet-02	34.91	33.43	151.26	421.51
SK-300-Wet-01	36.95	31.96	151.76	424.29
SK-300-Wet-02	36.69	36.95	151.70	487.26
SK-100-Acid-01	33.35	36.27	151.90	434.57
SK-100-Acid-02	33.07	34.94	152.00	422.21
SK-200-Acid-01	32.25	37.15	151.46	437.94
SK-200-Acid-02	36.27	38.17	151.64	496.21
SK-300-Acid-01	35.27	33.37	152.00	432.10
SK-300-Acid-02	35.62	34.67	151.84	447.76

Table 3.4 Phra Wihan specimens prepared for simulation of degradation and three-point bending test.

Specimen No.	Thickness, d (mm)	Width, b (mm)	Length (mm)	Weight (g)
PW-Initial-01	32.60	36.00	151.90	401.80
PW-Initial-02	34.95	32.50	151.85	400.17
PW-100-Dry-01	34.75	34.35	152.00	414.66
PW-100-Dry-02	34.35	34.35	152.00	417.70
PW-200-Dry-01	34.00	33.20	152.00	401.12
PW-200-Dry-02	33.30	31.70	152.35	384.53
PW-300-Dry-01	32.45	32.15	151.70	373.57
PW-300-Dry-02	33.95	35.75	152.30	425.30
PW-100-Wet-01	32.70	32.30	152.40	352.72
PW-100-Wet-02	33.80	33.05	151.85	395.54
PW-200-Wet-01	33.75	33.45	152.60	398.44
PW-200-Wet-02	31.10	29.55	151.50	328.59
PW-300-Wet-01	35.95	33.85	151.75	417.96
PW-300-Wet-02	34.60	33.90	151.80	415.20
PW-100-Acid-01	36.10	32.25	151.50	404.90
PW-100-Acid-02	35.40	32.05	151.45	390.86
PW-200-Acid-01	32.55	34.95	152.00	428.07
PW-200-Acid-02	33.55	34.85	152.40	414.72
PW-300-Acid-01	35.35	32.35	151.85	388.38
PW-300-Acid-02	34.45	32.70	152.10	388.19

3.2.3 Uniaxial compression test specimens

After three-point bending test, the specimens are spitted into 2 pieces, one is cut and ground to obtain flat ends with nominal dimensions of 35×35×70 mm^3 (Figure 3.3). They are subjected to uniaxial loading to obtain their unconfined compressive strength and elastic modulus.

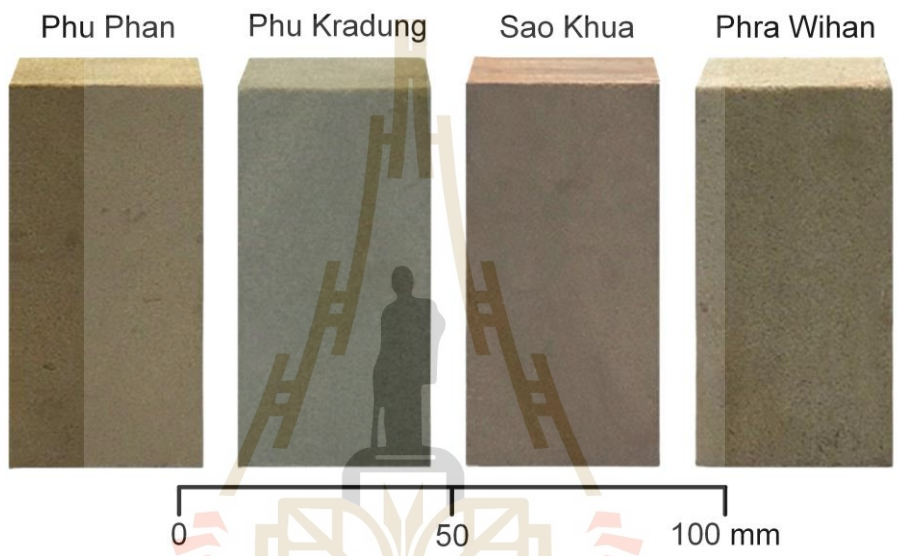

Figure 3.3 Some sandstone specimens prepared for uniaxial compression test.

3.2.4 X-ray diffraction tests

The other half of the prismatic specimens after subjecting to the three-point bending test, is ground to obtain powder with particle sizes of less than 0.25 mm (mesh #60) (Figure 3.4). The powder specimen is used to determine mineral compositions by X-ray diffraction (XRD) analysis.

Figure 3.4 Sandstone powder specimen prepared for XRD-diffraction analysis.

CHAPTER IV

LABORATORY TESTING

4.1 Introduction

This chapter describes the test specimens and methods for the rock degradation simulation. Three-point bending and uniaxial compression tests are also performed periodically. During of the specimens are measured. The densities compressive and tensile strength and deformation moduli are used as indicators for the degrees of degradation.

4.2 Simulation of rock degradation

Figure 4.1 shows the test cycles for the degradation simulation of the sandstone. The specimens for each sandstone type are first separated into three sets for the heating-cooling cycles to simulate the weathering environment. Nine specimens are used for each set (Figure 4.1). They are subjected to oven-heating at 105±5 °C for 12 hrs. Then, three specimens are air-cooled at 25±2 °C for 12 hrs. Three specimens are cooled by submerging in distilled water for 12 hrs. And the last three are submerged in sulfuric acid (with pH = 5.6) for 12 hrs. This acidic condition follows the annual precipitation in southeast Asia monitored by EANET (2016) from 2010 to 2014. The entire process is repeated for 300 cycles (300 days). Every 100 cycles, one specimen of each set is taken out of the test cycles. The rest of the specimens continues to subject to test cycles. The specimens that have been taken out every 100 cycles are subjected to physical, mechanical and mineralogical testing and compared with those of the initial condition (without subjecting to test cycle), of which test methods can be summarized below.

4.3 Specific gravity measurements

The density of the prismatic sandstone specimens is determined based on the ASTM C127-15 standard practice. The method involves weighting the specimen in the air and in distilled water.

The relative density (specific gravity) determined for each set specimen each condition is determined using the following relations

Relative density (specific gravity) = A/(B-C) (4.1)

where A is mass of oven-dry test sample in air, (g), B is mass of test sample in air, (g), and C is apparent mass of sample in water, (g).

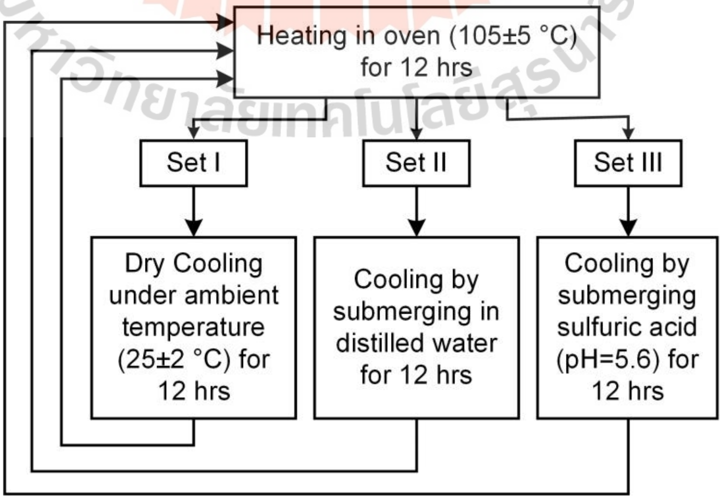

Figure 4.1 Heating-cooling cycles for three sets of specimens under 300 cycles.

4.4 Three-point bending tests

To obtain the initial tensile properties and the properties for every 100 test cycles, the specimens are subjected to three-point bending test (ASTM C293/C293M-16) to determine their bending tensile strength. Figure 4.2 shows the loading positions for the upper and lower bearing plates. A data logger (TC-32K) connected with the switching box is used to monitor the induced tensile strains from strain gage installed at the incipient crack initiation point (Figure 4.3). Its readings can provide tensile strains which can be later used to determine tensile deformation (elastic) modulus before failure. The induced tensile stress induced at the crack initiation point can be calculated by:

$$\sigma_t = 3PL/2bd^2 \tag{4.2}$$

where σ_t is tensile stresses, P is applied load, L is support span (140 mm), b is specimen width (35 mm), and d is specimen thickness (35 mm). The tensile elastic modulus for each specimen is determined from tangent of the stress-strain curves at 40% failure stress.

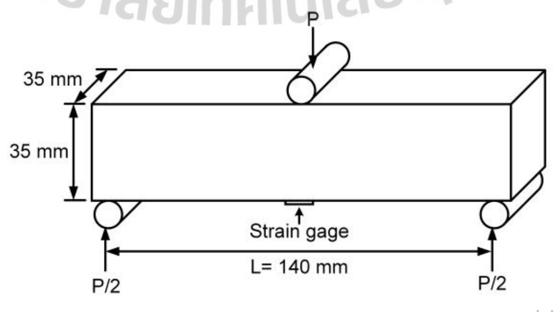

Figure 4.2 Test arrangement for three-point bending test

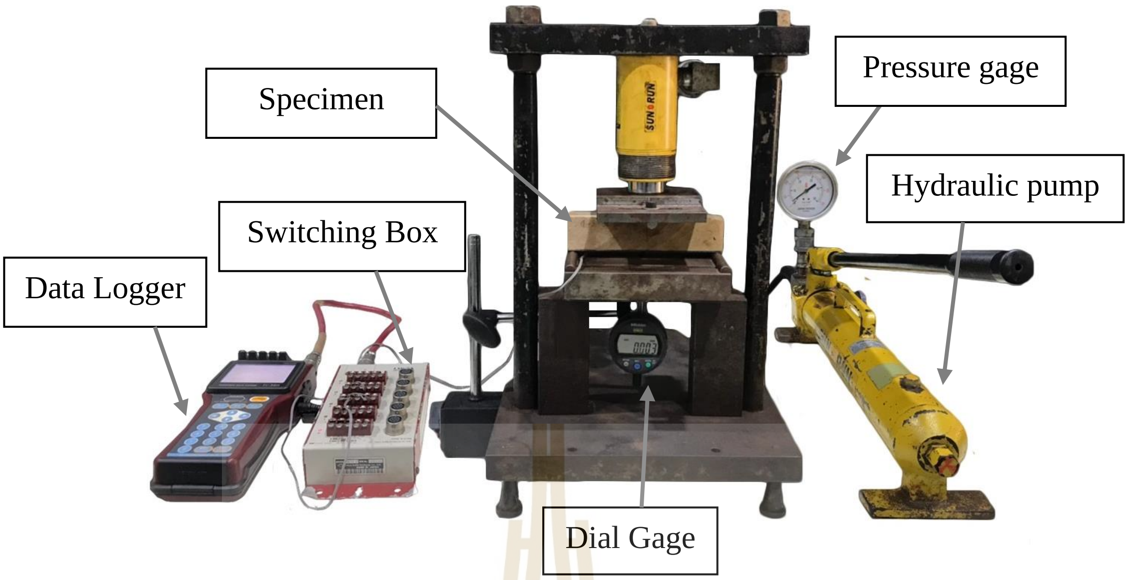

Figure 4.3 Three-point bending test apparatus.

4.5 Uniaxial compression tests

After the specimens are spitted into 2 pieces, one is cut to obtain flat ends with nominal dimensions of 35×35×70 mm^3. They are subjected to uniaxial loading to obtain their unconfined compressive strength and elastic modulus. The uniaxial compressive strength test method and calculation follow the ASTM D7012-14e1 standard practice. The testing performed by increasing the axial stress to the rock specimen. The dial gages installed to measure the axial and lateral strains. During the test, the axial strain and lateral strain will be monitored (Figure 4.4). The results used to determine the compressive strength, elastic modulus and Poisson's ratio and revealing the effect of rock degradation under initial condition and after every 100 test cycles.

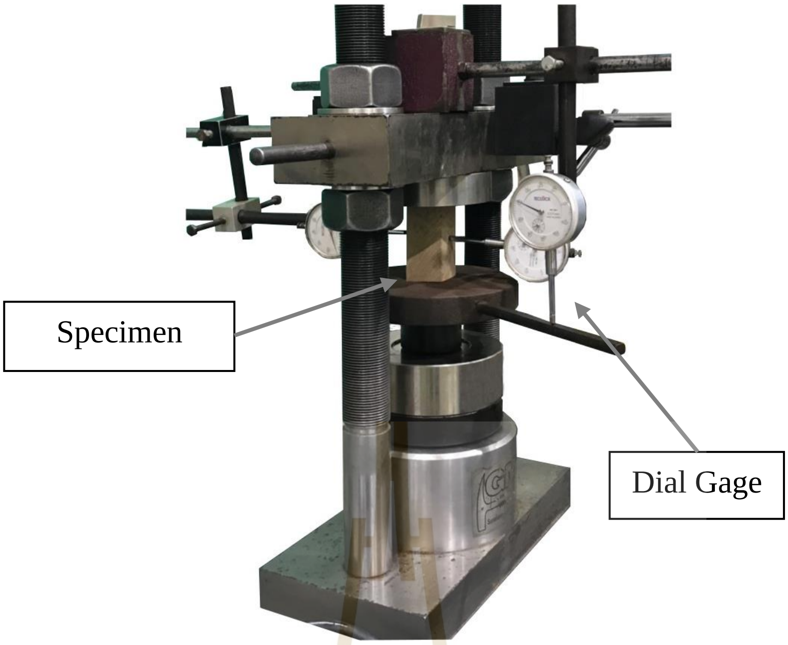

Figure 4.4 Uniaxial compression test arrangement.

4.6 X-ray diffraction tests

The other half of the prismatic specimens after subjecting to the three-point bending test, is ground to obtain powder with particle sizes of less than 0.25 mm (mesh #60). The specimen is used to determine mineral compositions by X-ray diffraction (XRD) analysis. The powder specimen is used to determine mineral compositions by X-ray diffractormeter-D2 phaser (Figure 4.5). X-ray powder diffraction is a method for determining the phase content of polycrystalline mineral. Every mineral exhibits a typical ‘X-ray fingerprint’, which is stored in databases This fingerprint is utilized in the DIFFRAC.EVA software for composition identification.

Figure 4.5 X-ray diffractormeter-D2 phaser.

CHAPTER V

TEST RESULTS

5.1 Introduction

This chapter describes the results of rock degradation simulations. The degrees of degradation are revealed by the changes of specimen specific gravity, compressive and tensile strengths and deformation moduli, and mineral compositions. These indicators have been monitored from the initial conditions through every 100 cycles of the simulations. Figures 5.1 through 5.4 show the pictures of the test specimens after subjecting to all test conditions.

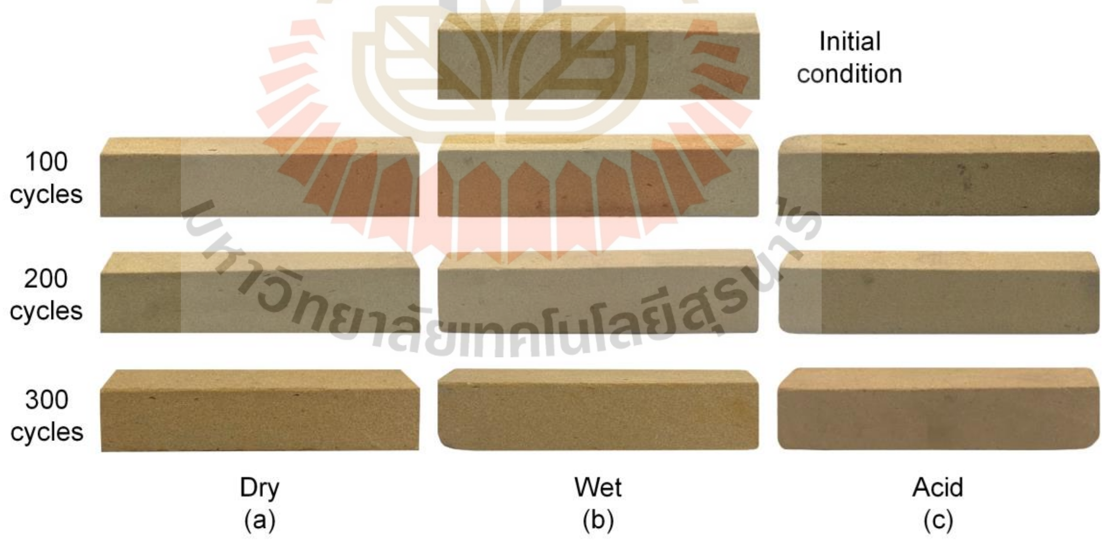

Figure 5.1 Picture of Phu Phan specimens through 100, 200 and 300 cycles under dry (a), wet (b) and acid (c) conditions.

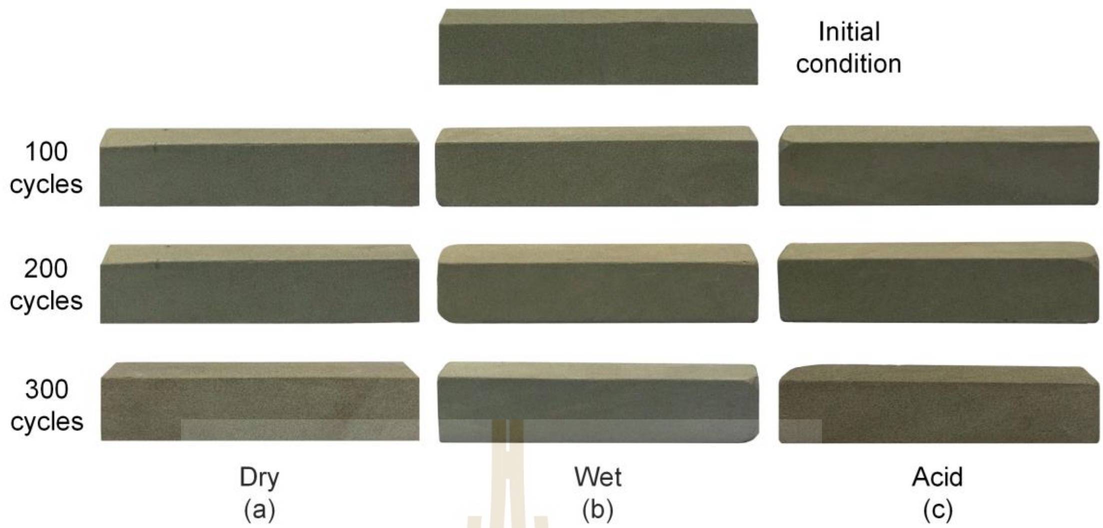

Figure 5.2 Picture of Phu Kradung specimens through 100, 200 and 300 cycles under dry (a), wet (b) and acid (c) conditions.

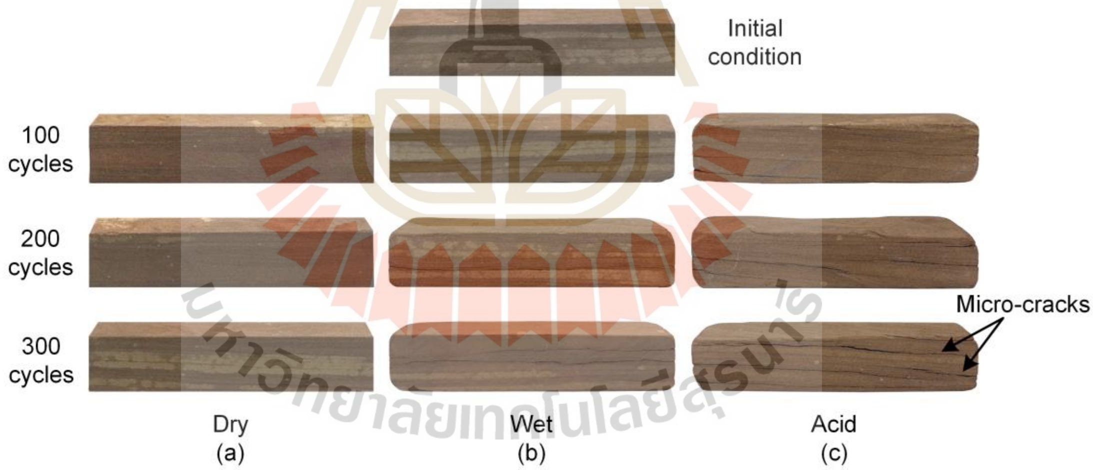

Figure 5.3 Picture of Sao Khua specimens through 100, 200 and 300 cycles under dry (a), wet (b) and acid (c) conditions.

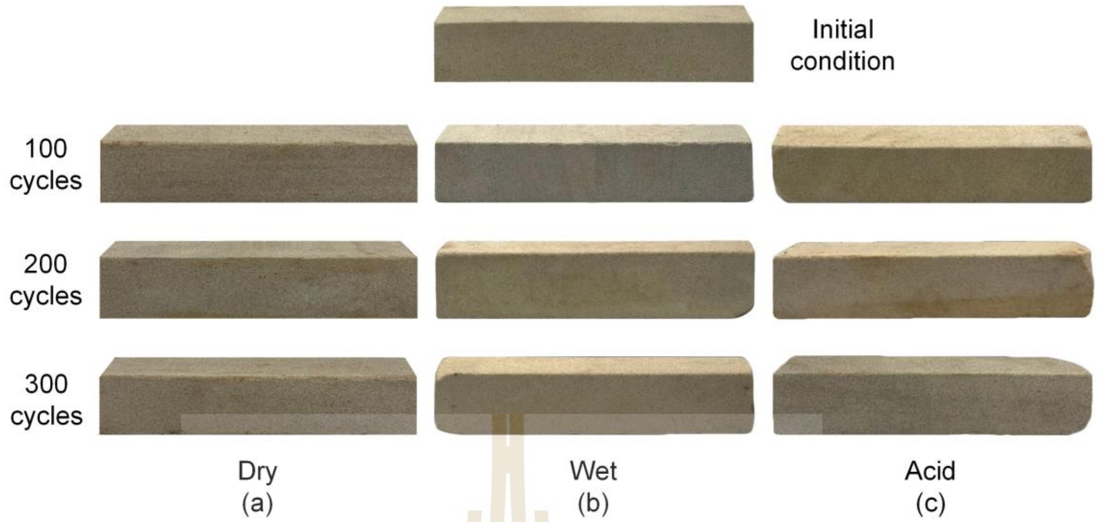

Figure 5.4 Picture of Phra Wihan specimens through 100, 200 and 300 cycles under dry (a), wet (b) and acid (c) conditions.

5.2 Specific gravity

The specific gravity values from the initial condition through the 300 cycles for all tested sandstones are given in Table 5.1. Figure 5.5 shows the rock specific gravities for all cooling conditions up to 300 test cycles. All sandstone types tend to be durable under heating-air cooling cycles. Water and acid can notably reduce the rock specific gravity. This may be due to that these liquids can dissolve the mineral compositions of the sandstones, and hence increases their pore spaces (porosity). Rock specimens that are cooled by submerging in acid show lower specific gravities than those in distilled water. All sandstone types pose similar reduction of the specific gravities as the number of test cycles (N) increases.

Table 5.1 Specific gravity of sandstone specimens.

Sandstone Type	Condition	Number of cycles			
		0	**100**	**200**	**300**
Phu Phan	Dry	2.40	2.40	2.39	2.39
	Wet		2.38	2.36	2.35
	Acid		2.36	2.34	2.33
Phu Kradung	Dry	2.53	2.52	2.52	2.52
	Wet		2.50	2.48	2.46
	Acid		2.48	2.46	2.44
Sao Khua	Dry	2.42	2.40	2.40	2.39
	Wet		2.35	2.33	2.30
	Acid		2.32	2.30	2.28
Phra Wihan	Dry	2.33	2.33	2.33	2.33
	Wet		2.31	2.30	2.29
	Acid		2.30	2.28	2.26

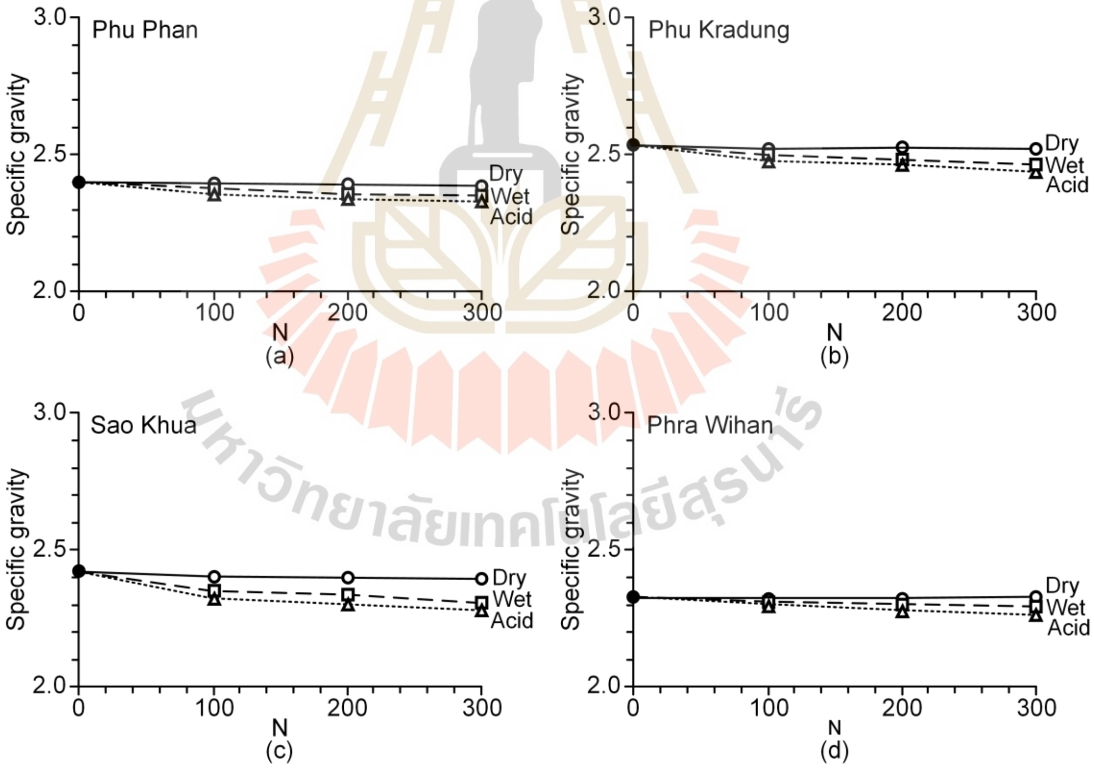

Figure 5.5 Specific gravity as a function of number of cycles (N) for Phu Phan (a), Phu Kradung (b), Sao Khua (c), and Phra Wihan (d) sandstones.

5.3 Compressive and tensile strength

Tables 5.2 and 5.3 give the compressive and tensile strengths of sandstone specimens after subjecting to 300 cycles under all cooling conditions. The effects of water and acid clearly show on the compressive and tensile strengths of the four sandstones, as shown in Figure 5.6. After 300 test cycles, the strength reduction is about 30-50% of the initial values. Under air-cooled (dry) conditions, the compressive and tensile strengths for the four sandstones tend to remain unchanged. This suggests that thermal loading up to 105 °C has not affected the mechanical properties of the tested sandstones.

Submerging in acid can reduce the rock strengths more than submerging in water. Sao Khua sandstone is highly sensitive to water and acid. After 100 cycles under acid cooling and 200 cycles under water cooling the specimens disintegrated along the bedding planes, and hence the compression testing can not be performed.

Table 5.2 Compressive strengths of sandstone specimens under all test conditions.

Rock Type	Condition	σ_c (MPa)			
		Number of cycles			
		0	100	200	300
Phu Phan	Dry	61.74	61.42	61.14	60.32
	Wet		55.06	50.69	47.17
	Acid		50.83	45.45	39.35
Phu Kradung	Dry	59.34	58.78	58.54	58.32
	Wet		51.85	45.20	35.01
	Acid		47.82	39.34	30.95
Sao Khua	Dry	56.91	56.74	56.25	55.58
	Wet		46.93	36.72	N/A
	Acid		34.52	N/A	N/A
Phra Wihan	Dry	54.45	54.41	54.34	54.29
	Wet		50.94	45.74	43.13
	Acid		43.63	35.57	31.97

Table 5.3 Tensile strengths of sandstone specimens under all test conditions.

Rock Type	Condition	σ_t (MPa)			
		Number of cycles			
		0	100	200	300
Phu Phan	Dry	15.27	14.76	14.63	14.44
	Wet		13.82	12.81	11.74
	Acid		12.28	11.39	10.19
Phu Kradung	Dry	13.99	13.57	13.55	13.14
	Wet		12.63	11.43	10.53
	Acid		11.57	10.43	8.47
Sao Khua	Dry	13.45	12.94	12.66	12.34
	Wet		10.00	7.34	5.63
	Acid		8.34	4.96	3.97
Phra Wihan	Dry	13.24	12.90	12.75	12.66
	Wet		11.29	10.10	8.86
	Acid		10.49	9.27	7.55

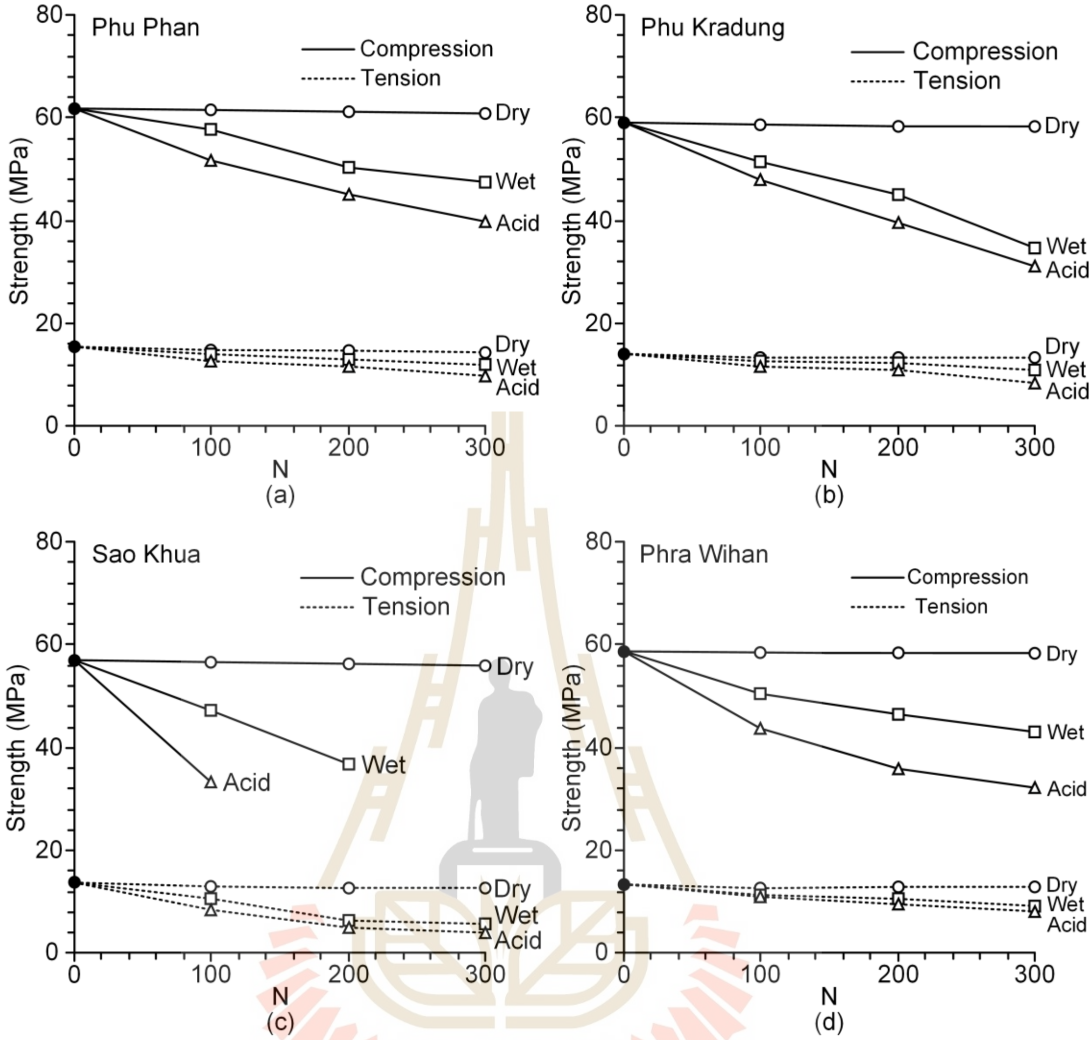

Figure 5.6 Compressive and tensile strengths as a function of number of cycles (N) for Phu Phan (a), Phu Kradung (b), Sao Khua (c), and Phra Wihan (d) sandstones.

5.4 Compressive and tensile deformation moduli

Figures 5.7 and 5.8 show the compressive and tensile stress-strains curves form start loading to failure for the uniaxial and three-point bending tests. The compressive and tensile deformation moduli have been measured form the tangent at about 40-50% of the peak stress. The results are given in Tables 5.4 and 5.5.

Similar to the strength reduction described in section 5.3, the effects of cooling by water and acid on the compressive and tensile deformation moduli of the sandstones can be clearly seen (Figure 5.9). For all sandstone types, the fluid submersion effects are more severe on the tensile moduli than the compressive moduli. The reduction of rock elastic moduli as the number of test cycles increase is more significant for the specimens that are cooled in acid than those in water. No significant change of the compressive and tensile deformation moduli has been observed for the specimens that subject to air-cooled (dry) condition. This coincides with the observed strengths described earlier.

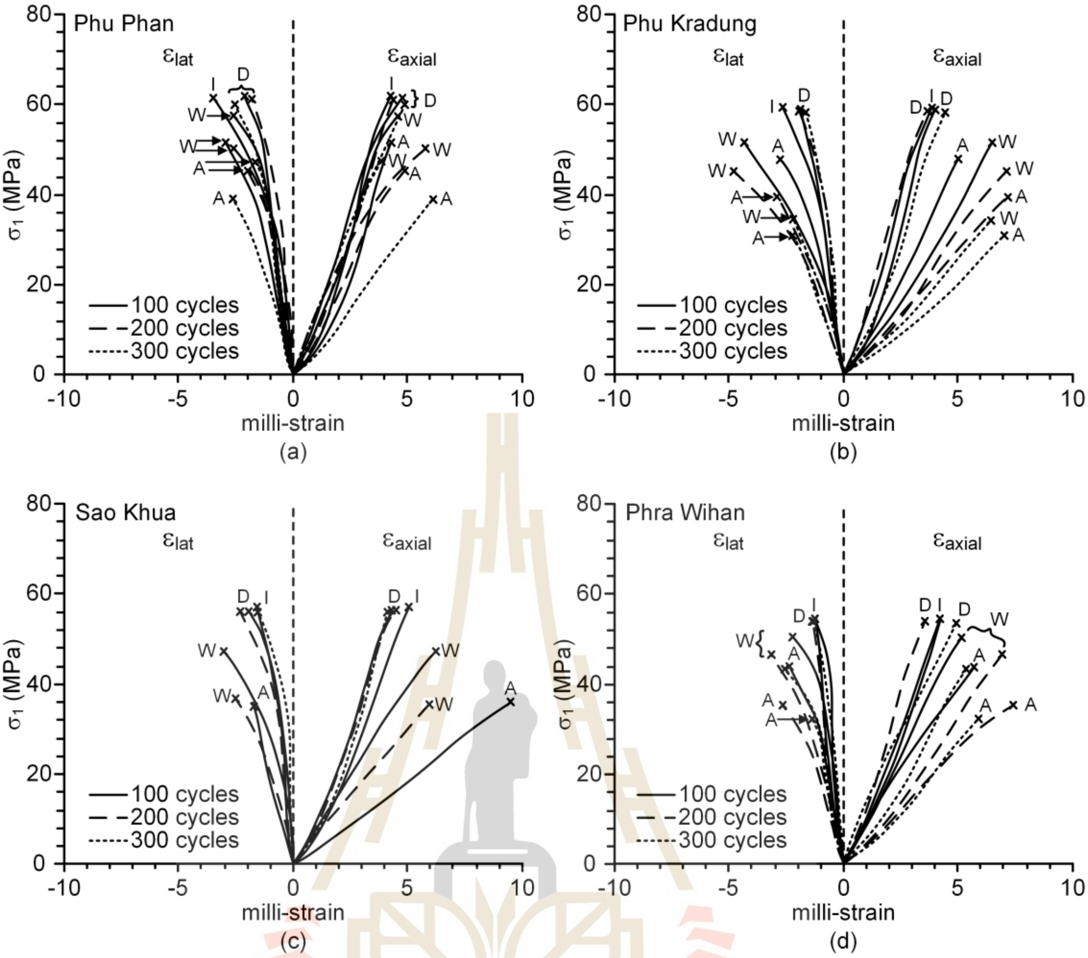

Figure 5.7 Stress-strain curve from uniaxial compression tests for Phu Phan (a), Phu Kradung (b), Sao Khua (c), and Phra Wihan (d) sandstones under initial (I), dry (D), wet (W), and acid (A) condition.

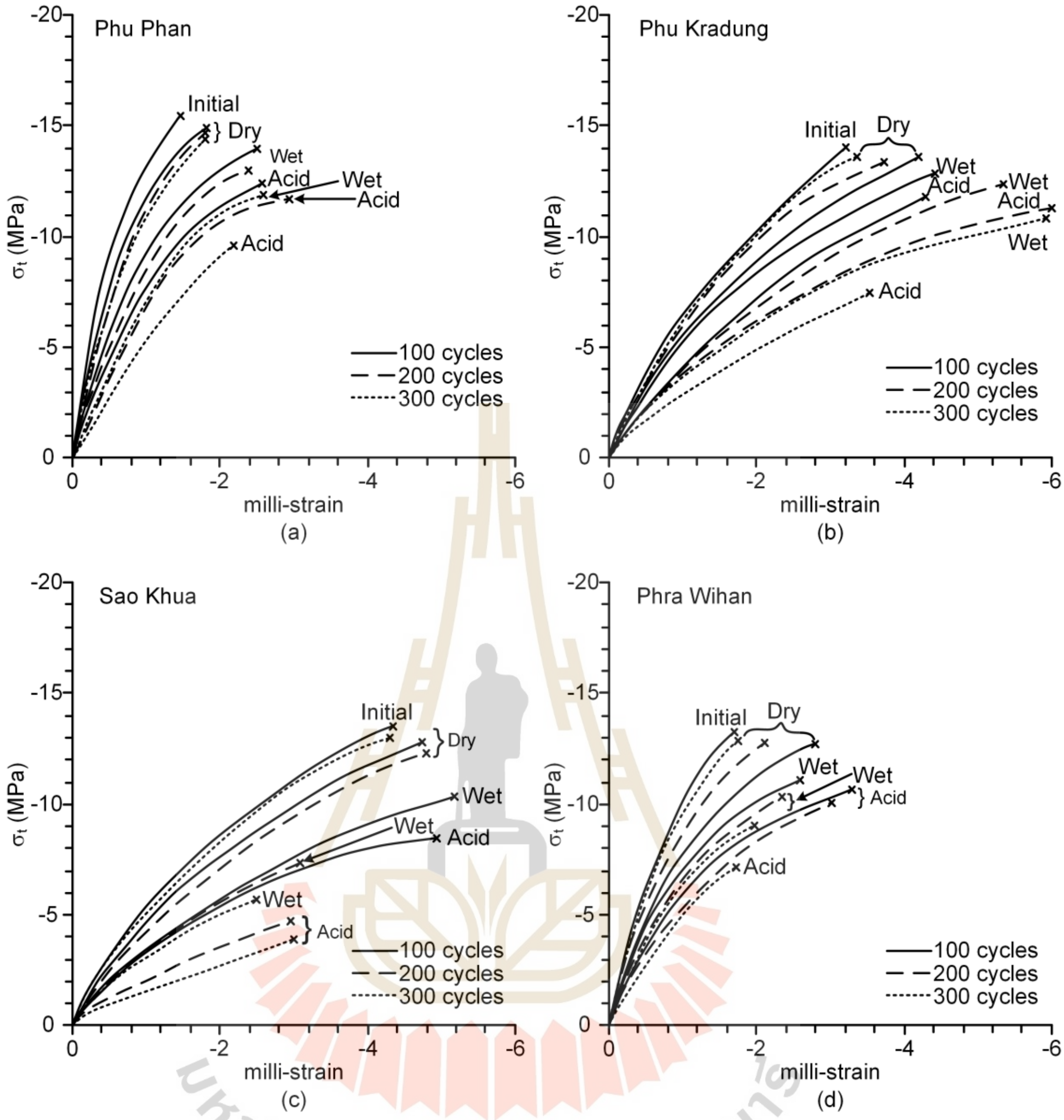

Figure 5.8 Stress-strain curve from three-point bending tests for Phu Phan (a), Phu Kradung (b), Sao Khua (c), and Phra Wihan (d) sandstones.

Table 5.4 Compressive elastic modulus of sandstone specimens under all test condition.

Rock Type	Condition	E_c (MPa)			
		Number of cycles			
		0	100	200	300
Phu Phan	Dry	19.00	18.81	18.48	18.33
	Wet		14.23	11.77	9.67
	Acid		11.33	9.69	7.61
Phu Kradung	Dry	14.95	14.73	14.29	14.02
	Wet		8.75	7.73	5.53
	Acid		7.30	5.67	3.40
Sao Khua	Dry	12.75	12.23	11.54	11.31
	Wet		7.79	5.92	N/A
	Acid		2.48	N/A	N/A
Phra Wihan	Dry	13.69	13.28	13.08	13.05
	Wet		10.68	8.80	7.15
	Acid		8.42	7.48	5.73

Table 5.5 Tensile elastic modulus strength of sandstone specimens under all test condition.

Sandstone Type	Condition	E_t (MPa)			
		Number of cycles			
		0	100	200	300
Phu Phan	Dry	13.51	13.28	12.23	13.19
	Wet		10.46	8.80	7.79
	Acid		6.97	5.99	5.08
Phu Kradung	Dry	6.82	6.50	6.35	6.29
	Wet		4.99	3.58	2.69
	Acid		3.58	2.50	2.02
Sao Khua	Dry	5.43	5.36	5.29	5.21
	Wet		3.07	2.52	1.97
	Acid		1.98	1.69	1.16
Phra Wihan	Dry	9.56	0.09	8.69	8.32
	Wet		7.00	6.48	6.07
	Acid		5.42	4.19	3.91

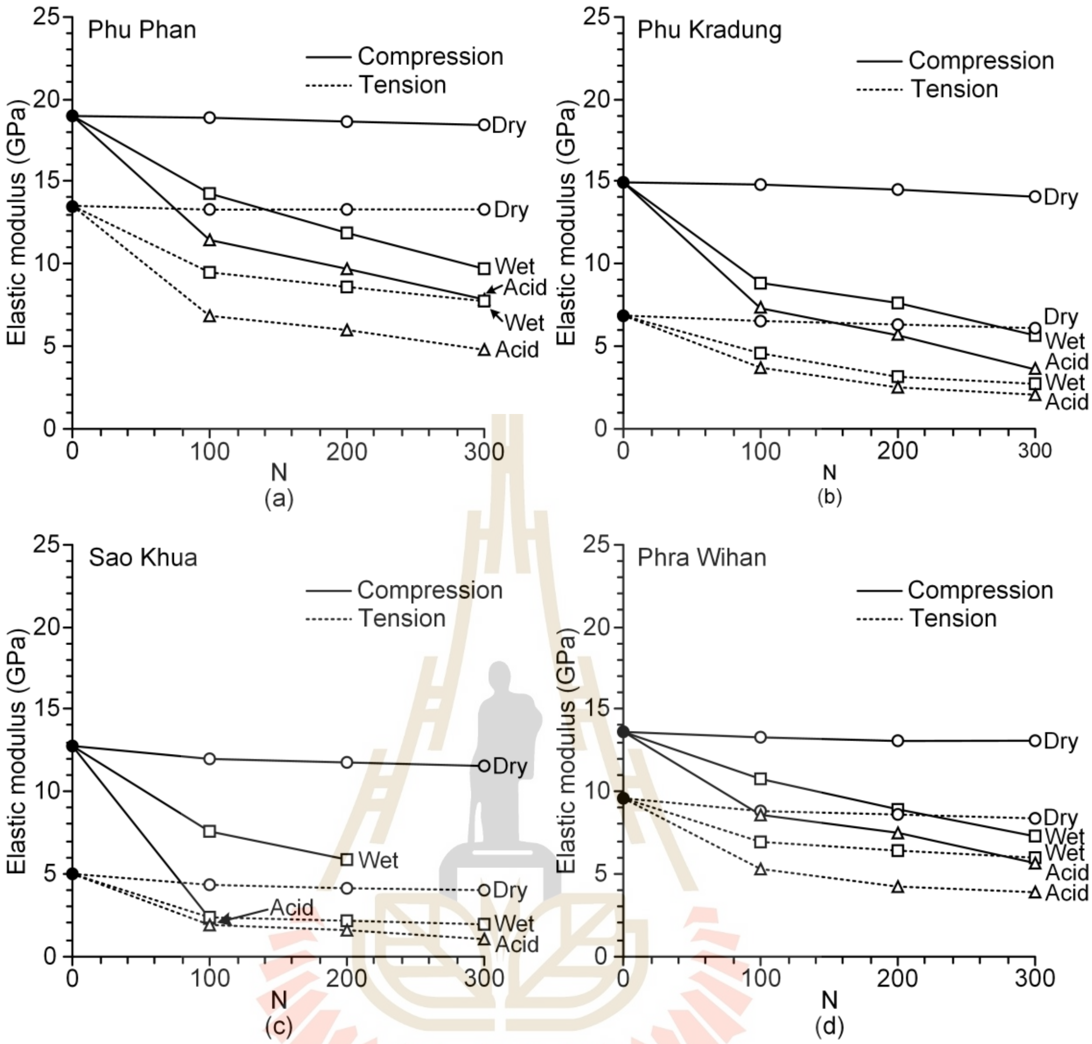

Figure 5.9 Elastic moduli as a function of number of cycles (N) for Phu Phan (a), Phu Kradung (b), Sao Khua (c), and Phra Wihan (d) sandstones.

5.5 Poisson's ratio

Along with the deformation modulus measurements, the Poisson's ratios of the sandstone specimens after subjecting to every 100 test cycles have been calculated from the uniaxial compression tests. Table 5.6 gives the results. Submerging in liquids to cool the specimens increases their Poisson's ratios, as also indicated in Figure 5.10. The Poisson's ratio is determined by the ratio of lateral expansion-to-axial contraction during axial loading of the uniaxial compression test. For all sandstone types, the Poisson's ratio increases with the test cycles. Slight increase is observed when the specimens are air-cooled (dry condition). Specimens that are submerged in acid dilate laterally more than those in water.

Table 5.6 Poisson's ratios of sandstone specimens under all test conditions.

Sandstone Type	Condition	ν (MPa)			
		Number of cycles			
		0	100	200	300
Phu Phan	Dry	0.22	0.22	0.23	0.23
	Wet		0.24	0.27	0.28
	Acid		0.27	0.28	0.30
Phu Kradung	Dry	0.24	0.25	0.26	0.26
	Wet		0.29	0.30	0.31
	Acid		0.30	0.32	0.33
Sao Khua	Dry	0.23	0.24	0.25	0.25
	Wet		0.31	0.32	N/A
	Acid		0.33	N/A	N/A
Phra Wihan	Dry	0.25	0.25	0.26	0.27
	Wet		0.28	0.29	0.31
	Acid		0.30	0.31	0.32

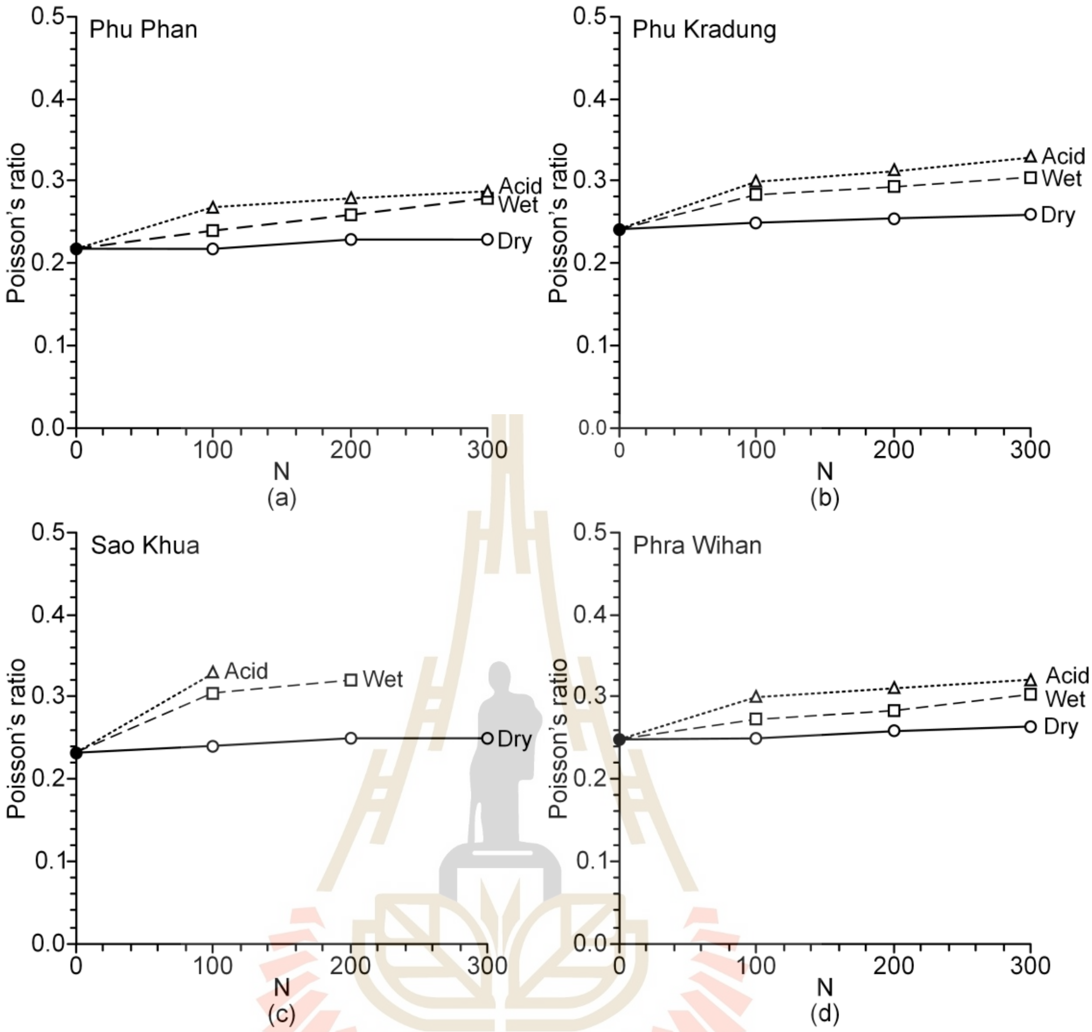

Figure 5.10 Poisson's ratio as a function of number of test cycles (N) for Phu Phan (a), Phu Kradung (b), Sao Khua (c), and Phra Wihan (d) sandstones.

5.6 Equivalent quartz contents

Forty specimens have been prepared and analyzed by XRD to determine their mineral compositions in weight percent. Table 5.7 gives the results. Quartz represents the largest percentages for all sandstone types under all test cycles and conditions. The rest of the minerals represent other minerals less durable. Direct comparison of the mineral contents among different test conditions and cycles is difficult. This is because both quartz and other minerals are lost during the test cycles. The ratios of quartz-to-other mineral (called here as equivalent quartz content, Moradizadeh et al., (2016)) are, therefore, proposed. They are plotted as a function of test cycles in Figure 5.11. Table 5.8 gives their numerical values for all sandstone types. The equivalent quartz content (Q_e) increases with the test cycles, particularly those that are submerged in acid. Slight increase has been observed for those that are cooled under dry condition. This supports the previous postulation that cooling the sandstone specimens in liquid can dissolve other minerals which results in an increase of their porosity (density decrease).

Table 5.7 Mineral compositions of sandstone specimens.

Sandstone type	Conditions	Number of cycles	Mineral compositions (%)								
			Quartz	Kaolinite	Muscovite	Albite	Anorthite	Microcline	Calcite	Oligoclase	Chlorite
Phu Phan	Initial	0	84.94	2.94	3.89	1.55	0.00	1.20	0.03	0.00	5.45
	Dry	100	85.18	1.68	3.37	0.25	1.27	0.62	0.04	0.89	6.70
		200	85.66	8.94	1.89	0.21	0.72	1.46	0.04	0.00	1.08
		300	85.75	6.45	0.92	2.23	0.04	0.00	0.07	0.00	4.16
	Wet	100	86.75	6.02	1.37	0.40	0.82	1.91	0.00	0.00	2.66
		200	86.93	2.56	4.12	0.09	0.10	1.24	0.41	0.00	4.96
		300	87.32	5.12	2.27	1.47	0.23	0.76	0.07	0.00	2.42
	Acid	100	88.32	3.41	2.66	0.02	1.92	0.09	0.00	0.00	1.37
		200	88.77	4.34	2.35	1.21	0.13	0.55	0.05	0.06	2.12
		300	88.95	1.11	3.74	0.65	0.11	0.07	0.16	0.00	4.34
Phu Kradung	Initial	0	35.15	2.94	9.36	22.1	2.89	4.69	0.26	13.0	9.51
	Dry	100	35.34	1.00	6.59	5.46	5.70	2.50	1.60	27.3	14.46
		200	36.20	5.50	2.13	20.6	10.4	6.05	1.30	3.33	14.43
		300	37.23	3.92	7.45	23.5	5.56	10.5	0.00	2.61	9.20
	Wet	100	37.65	3.82	6.33	25.2	6.81	7.21	0.76	1.33	10.89
		200	40.16	1.11	4.47	29.1	2.65	4.58	0.87	1.05	16.01
		300	40.37	6.69	2.45	21.1	1.03	8.75	0.15	4.82	14.63
	Acid	100	40.95	1.25	1.25	33.8	1.07	5.70	0.32	2.60	1.77
		200	40.97	7.11	7.11	23.0	0.92	10.5	0.06	2.46	13.73
		300	45.71	3.03	3.03	18.6	7.46	10.1	0.71	0.78	12.77
Sao Khua	Initial	0	34.17	3.07	11.0	33.2	3.52	4.56	0.17	2.66	7.58
	Dry	100	37.23	3.92	7.45	23.5	5.56	10.5	0.00	2.62	9.19
		200	37.29	0.45	7.84	30.5	3.65	9.60	0.10	5.26	5.29
		300	37.63	0.48	8.43	30.4	4.72	11.4	0.49	2.21	4.19
	Wet	100	38.34	0.26	10.8	25.0	8.84	8.13	0.00	2.73	5.81
		200	38.47	0.52	11.6	26.7	4.23	8.72	0.00	4.09	5.59
		300	38.69	0.70	10.5	29.9	1.86	9.25	0.03	4.32	4.67
	Acid	100	38.76	0.58	10.1	30.8	2.08	6.88	0.30	4.56	5.78
		200	42.19	2.06	5.77	35.8	1.62	3.56	0.00	3.53	5.47
		300	42.40	2.59	8.94	27.0	3.43	9.39	0.20	2.04	3.95

Table 5.7 Mineral compositions of sandstone specimens. (count.)

Sandstone type	Conditions	Number of cycles	Quartz	Kaolinite	Muscovite	Albite	Anorthite	Microcline	Calcite	Oligoclase	Chlorite
			Mineral compositions (%)								
Phra Wihan	Initial	0	82.84	3.41	3.44	0.79	1.07	3.31	0.31	0.00	4.83
	Dry	100	84.48	11.32	0.24	2.25	0.28	0.73	0.05	0.00	0.65
		200	84.93	3.19	1.54	0.00	2.47	2.81	0.10	0.00	4.96
		300	85.30	2.62	3.94	0.40	0.94	1.53	0.05	0.00	5.22
	Wet	100	86.88	2.97	2.84	0.02	2.02	1.51	0.04	0.00	3.72
		200	87.34	2.77	1.92	0.85	2.30	1.66	0.54	0.00	2.62
		300	88.98	2.20	2.81	0.68	1.78	0.69	0.06	0.00	2.80
	Acid	100	89.01	8.74	0.20	1.28	0.15	0.18	0.05	0.04	0.35
		200	90.57	1.45	1.60	0.00	3.38	1.08	0.11	0.00	1.81
		300	91.49	1.86	2.49	0.36	1.24	0.32	0.06	0.02	2.16

Table 5.8 Equivalent quartz contents of sandstone specimens under all test conditions.

Sandstone Type	Condition	Equivalent quartz content, Q_e			
		Number of cycles			
		0	100	200	300
Phu Phan	Dry	5.64	5.75	5.95	6.02
	Wet		6.55	6.65	6.89
	Acid		7.56	7.90	8.05
Phu Kradung	Dry	0.54	0.55	0.57	0.59
	Wet		0.60	0.67	0.68
	Acid		0.69	0.69	0.84
Sao Khua	Dry	0.52	0.59	0.59	0.60
	Wet		0.62	0.63	0.63
	Acid		0.63	0.73	0.74
Phra Wihan	Dry	4.83	5.44	5.64	5.80
	Wet		6.62	6.90	8.07
	Acid		8.10	9.60	10.75

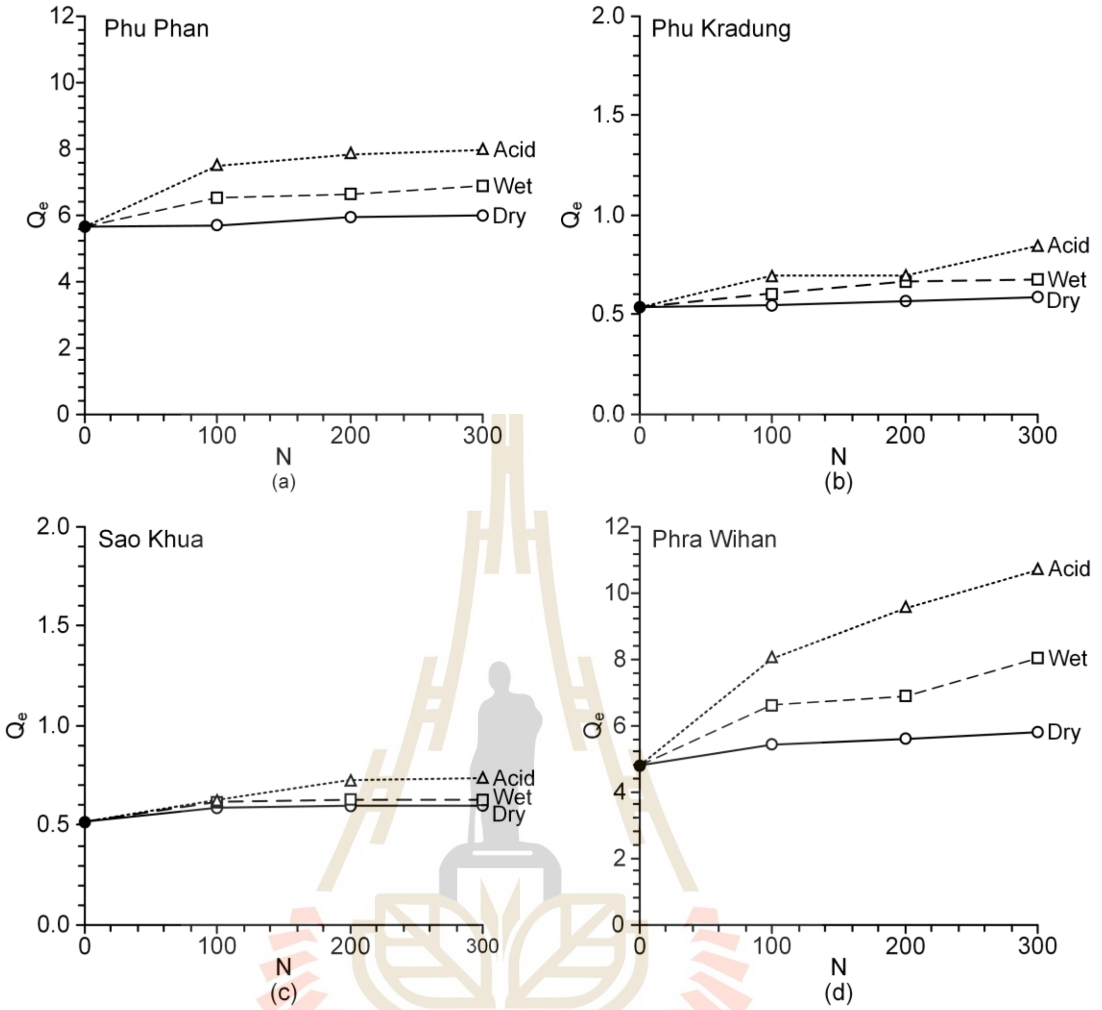

Figure 5.11 Equivalent quartz content (Q_e) as a function of number of test cycles (N) for Phu Phan (a), Phu Kradung (b), Sao Khua. (c), and Phra Wihan (d) sandstones.

CHAPTER VI

ANALYSIS OF TEST RESULTS

6.1 Introduction

The objective of this chapter is to mathematically define the weathering parameters, including specific gravity, compressive and tensile strength, compressive and tensile deformation moduli, and Poisson's ratio as a function of time. The results are used to predict the weathering conditions of the rocks beyond the durations used in this study.

6.2 Specific gravity

Figure 6.1 plots the specific gravity as a function number of cycles (N) from the initial condition through the 300 cycles for all tested sandstones. Regression analyses on the specific gravity values indicate that a polynomial equation can best describe the variation of SG with N. The specific gravity of all sandstone types decreases with the increase in number of cycles. Rock specimens that are cooled by submerging in acid show lower specific gravities than those in distilled water. Table 4.4 gives results of regression analysis and the empirical relation between SG and N for all rock types. The coefficients of correlation (R^2) are very good.

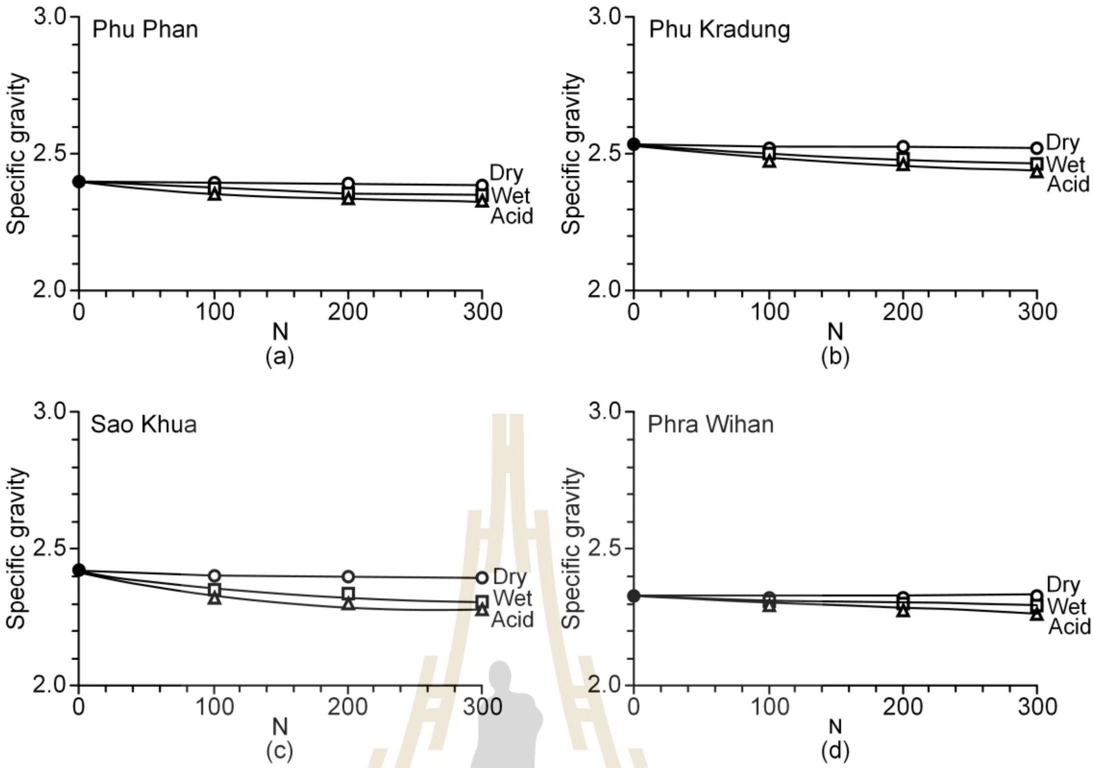

Figure 6.1 The relationship curve between specific gravity and number of cycles (N) for Phu Phan (a), Phu Kradung (b), Sao Khua (c), and Phra Wihan (d) sandstones.

Table 6.1 Empirical constants for a polynomial relationship between SG and N.

Sandstone Type	Condition	$SG_{(N)} = \alpha_{SG}N^2 - \beta_{SG}N + SG_0$		Correlation Coefficients
		α_{SG}	β_{SG}	
Phu Phan	Dry	4×10^{-8}	6×10^{-5}	0.9785
	Wet	5×10^{-7}	0.0003	0.9883
	Acid	9×10^{-7}	0.0005	0.9943
Phu Kradung	Dry	1×10^{-7}	7×10^{-5}	0.9761
	Wet	5×10^{-7}	0.0004	0.9987
	Acid	7×10^{-7}	0.0005	0.9638
Sao Khua	Dry	3×10^{-7}	0.0002	0.9824
	Wet	1×10^{-6}	0.0007	0.9547
	Acid	2×10^{-6}	0.0010	0.9722
Phra Wihan	Dry	2×10^{-8}	2×10^{-5}	0.9887
	Wet	2×10^{-7}	0.0002	0.9809
	Acid	9×10^{-8}	0.0002	0.9957

Notes: α_{SG} and β_{SG} are empirical constants

N is number of test cycle

SG_0 represents the specific gravity at initial conditions

6.3 Compressive and tensile strength

The compressive and tensile strengths of sandstone specimens under all cooling condition decrease as the number of test cycles increase, as shown in Figures 6.2 and 6.3. For all sandstone types, variation of the compressive and tensile strengths with number of cycles can be best represented by a polynomial equation. The compressive and tensile strengths under acid cooling decrease at a faster rate, as compared to that of the cooled by water. Tables 6.2 and 6.3 show the empirical constants of the polynomial equation for the four sandstones. Very good correlations are obtained (R^2 > 0.9)

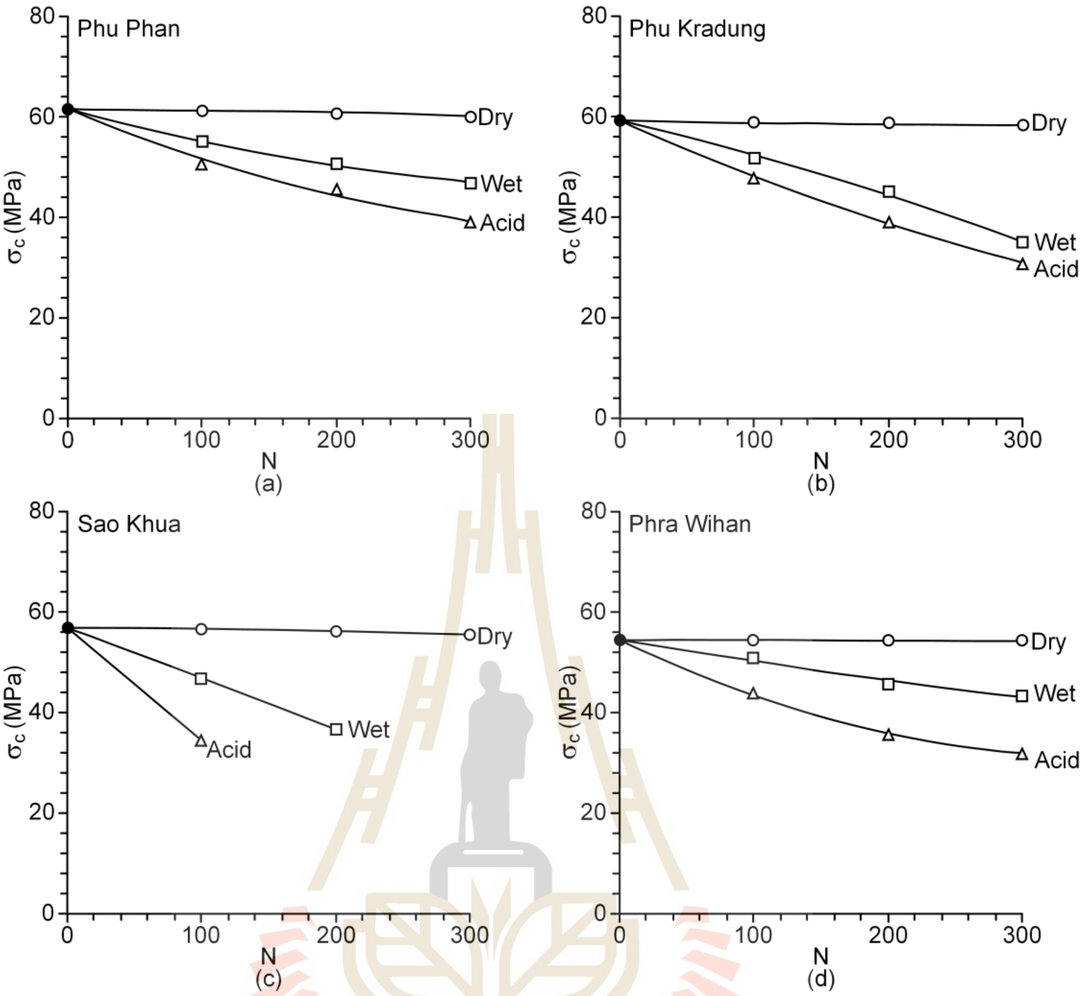

Figure 6.2 The relationship curve between compressive strength and number of cycles (N) for Phu Phan (a), Phu Kradung (b), Sao Khua (c), and Phra Wihan (d) sandstones.

Table 6.2 Empirical constants for a polynomial relationship between σ_c and N.

Sandstone Type	Condition	$\sigma_{c,(N)} = \alpha_c N^2 - \beta_c N + \sigma_{c,0}$		Correlation Coefficients
		α_c	β_c	
Phu Phan	Dry	-1×10^{-5}	0.0012	0.9840
	Wet	8×10^{-5}	0.0726	0.9990
	Acid	0.0001	0.1121	0.9924
Phu Kradung	Dry	9×10^{-6}	0.0060	0.9926
	Wet	-6×10^{-5}	0.0618	0.9968
	Acid	8×10^{-5}	0.1181	0.9990
Sao Khua	Dry	-1×10^{-5}	0.0007	0.9989
	Wet	-1×10^{-5}	0.0986	1
	Acid	0	0.2239	1
Phra Wihan	Dry	-2×10^{-7}	0.0005	0.9858
	Wet	2×10^{-5}	0.0435	0.9876
	Acid	0.0002	0.1288	0.9995

Notes: α_c and β_c are empirical constants

N is number of test cycle

$\sigma_{c,0}$ represents the compressive strength at initial conditions

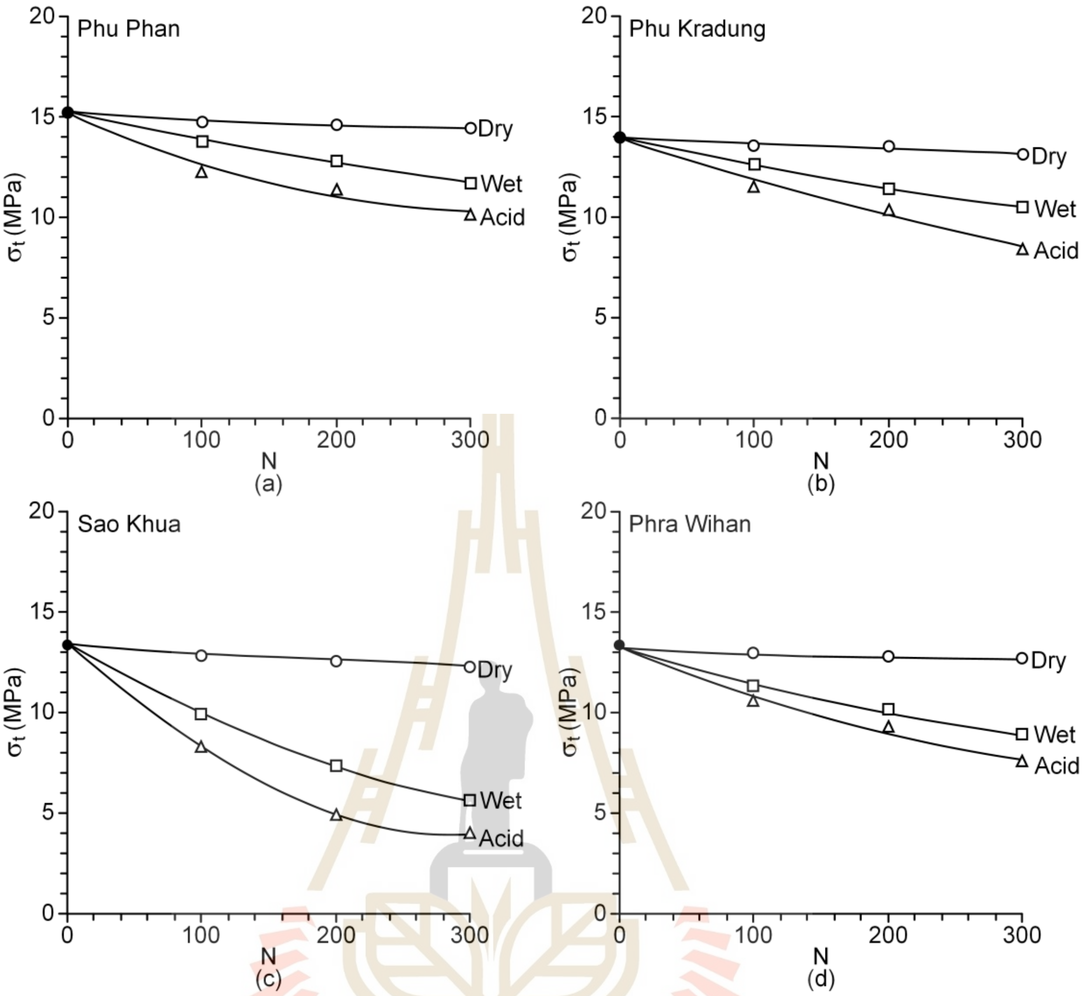

Figure 6.3 The relationship curve between tensile strength and number of cycles (N) for Phu Phan (a), Phu Kradung (b), Sao Khua (c), and Phra Wihan (d) sandstones.

Table 6.3 Empirical constants for a polynomial relationship between σ_t and N.

Sandstone Type	Condition	$\sigma_{t,(N)} = \alpha_t N^2 - \beta_t N + \sigma_{t,0}$		Correlation Coefficient
		α_t	β_t	
Phu Phan	Dry	8×10^{-6}	0.0052	0.9727
	Wet	1×10^{-5}	0.0147	0.9979
	Acid	5×10^{-5}	0.0309	0.9785
Phu Kradung	Dry	2×10^{-6}	0.0032	0.9091
	Wet	1×10^{-5}	0.0150	0.9999
	Acid	1×10^{-5}	0.0223	0.9857
Sao Khua	Dry	5×10^{-6}	0.0052	0.9936
	Wet	4×10^{-5}	0.0391	1
	Acid	0.0001	0.0624	0.9996
Phra Wihan	Dry	6×10^{-6}	0.0039	0.9940
	Wet	2×10^{-5}	0.0201	0.9968
	Acid	3×10^{-5}	0.0272	0.9873

Notes: α_t and β_t are empirical constants

N is number of test cycle

$\sigma_{t,0}$ represents the tensile strength at initial conditions

6.4 Compressive and tensile deformation moduli

All sandstone types pose reduction of the compressive and tensile deformation moduli similar to the compressive and tensile strength, as the number of test cycles (N) increases (Figures 6.4 and 6.5). The compressive and tensile deformation moduli of sandstone specimens that are subjected to water and acid cooling cycles are lower than those subjected to air cooling cycles. Under air-cooled (dry) condition, the compressive and tensile deformation moduli as the number of cycles is not significant change. The empirical constants in the polynomial equation for each sandstone type are shown in Tables 6.4 and 6.5, with the correlation coefficients of greater than 0.9.

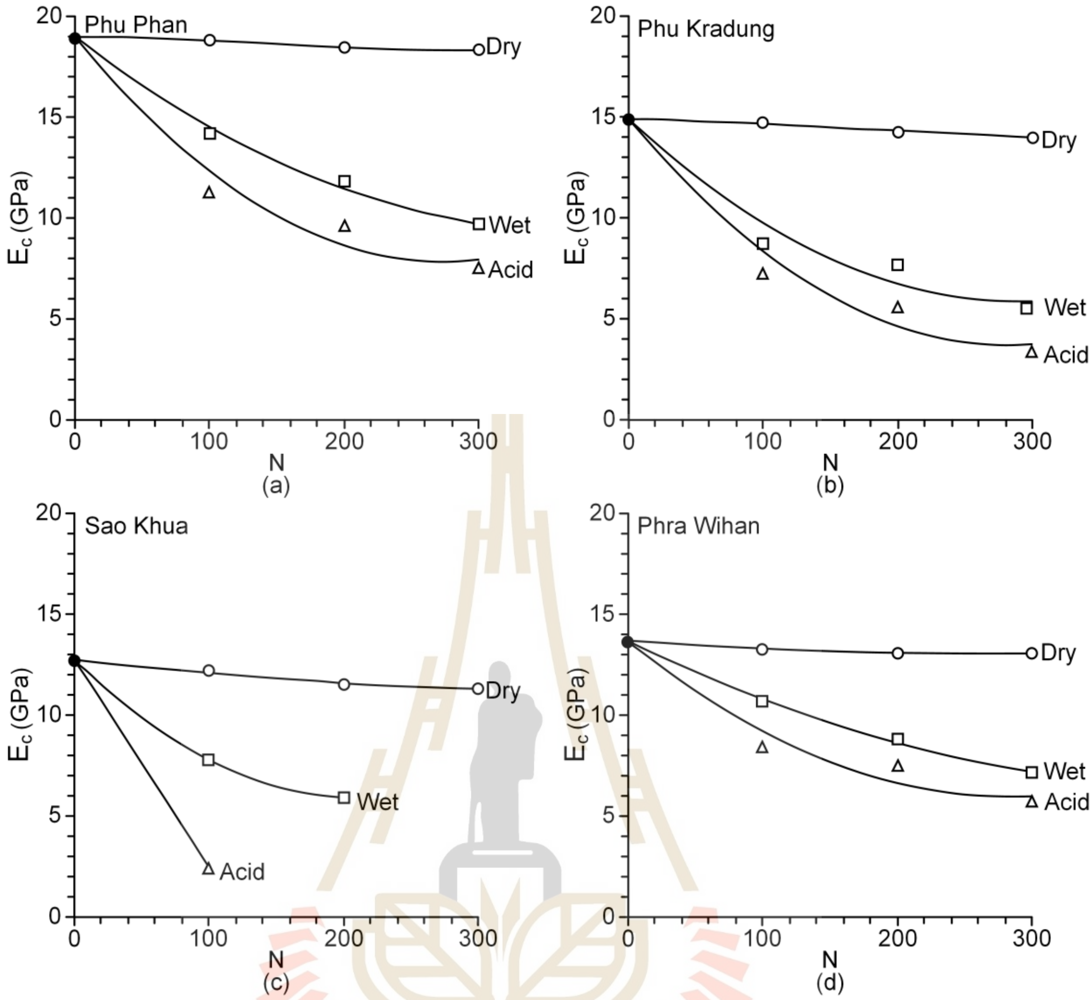

Figure 6.4 The relationship curve between compressive elastic modulus and number of cycles (N) for Phu Phan (a), Phu Kradung (b), Sao Khua (c), and Phra Wihan (d) sandstones.

Table 6.4 Empirical constants for a polynomial relationship between E_c and N.

Sandstone Type	Condition	$E_{c,(N)} = \alpha_{E,c}N^2 - \beta_{E,c}N + E_{c,0}$		Correlation Coefficients
		$\alpha_{E,c}$	$\beta_{E,c}$	
Phu Phan	Dry	7×10^{-7}	0.0025	0.9790
	Wet	7×10^{-5}	0.0516	0.9958
	Acid	0.0001	0.0814	0.9702
Phu Kradung	Dry	2×10^{-6}	0.0027	0.9860
	Wet	0.0001	0.0628	0.9567
	Acid	0.0001	0.0803	0.9691
Sao Khua	Dry	7×10^{-6}	0.0069	0.9832
	Wet	0.0002	0.0651	1
	Acid	0	0.1028	1
Phra Wihan	Dry	1×10^{-5}	0.0050	0.9999
	Wet	4×10^{-5}	0.0323	0.9982
	Acid	9×10^{-5}	0.0541	0.9605

Notes: $\alpha_{E,c}$ and $\beta_{E,c}$ are empirical constants

N is number of test cycle

$E_{c,0}$ represents the compressive elastic modulus at initial conditions

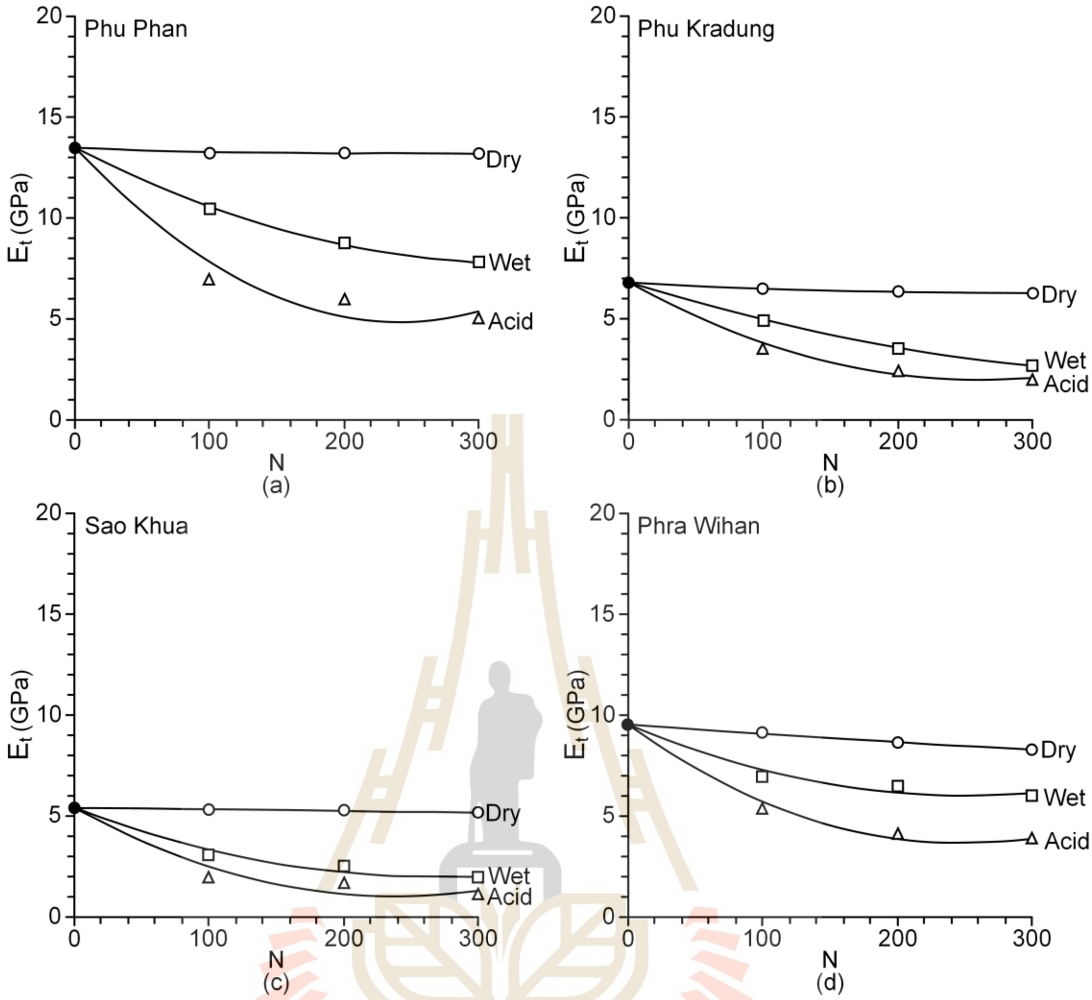

Figure 6.5 The relationship curve between tensile elastic modulus and number of cycles (N) for Phu Phan (a), Phu Kradung (b), Sao Khua (c), and Phra Wihan (d) sandstones.

Table 6.5 Empirical constants for a polynomial relationship between E_t and N.

Sandstone Type	Condition	$E_{t,(N)} = \alpha_{E,t}N^2 - \beta_{E,t}N + E_{t,0}$		Correlation Coefficients
		α	β	
Phu Phan	Dry	5×10^{-6}	0.0025	0.9743
	Wet	5×10^{-5}	0.0346	0.9984
	Acid	0.0001	0.0715	0.9641
Phu Kradung	Dry	7×10^{-6}	0.0037	0.9980
	Wet	2×10^{-5}	0.0208	0.9999
	Acid	7×10^{-5}	0.0371	0.9907
Sao Khua	Dry	2×10^{-7}	0.0007	0.9998
	Wet	5×10^{-5}	0.0255	0.9751
	Acid	8×10^{-5}	0.0369	0.9460
Phra Wihan	Dry	3×10^{-6}	0.0049	0.9999
	Wet	6×10^{-5}	0.0282	0.9738
	Acid	1×10^{-4}	0.0482	0.9899

Notes: $\alpha_{E,t}$ and $\beta_{E,t}$ are empirical constants

N is number of test cycle

$E_{t,0}$ represents the tensile elastic modulus at initial conditions

6.5 Poisson's ratio

The relationship curve between Poisson's ratio and number of test cycles in Figure 6.6. The Poisson's ratio under different numbers of cycles for each sandstone type can be represented by a polynomial equation. All sandstone types show the Poisson's ratio increases with increasing number of heating-cooling cycles. Submerging rock specimens under distilled water and acid induce higher rates of increasing the Poisson's ratio than under air-cooled. This is probably due to that these water and acid can dissolve another mineral durable less than quartz, and therefore decreasing its specific gravity. Table 6.6 lists the empirical constants in the polynomial equation for the four sandstones.

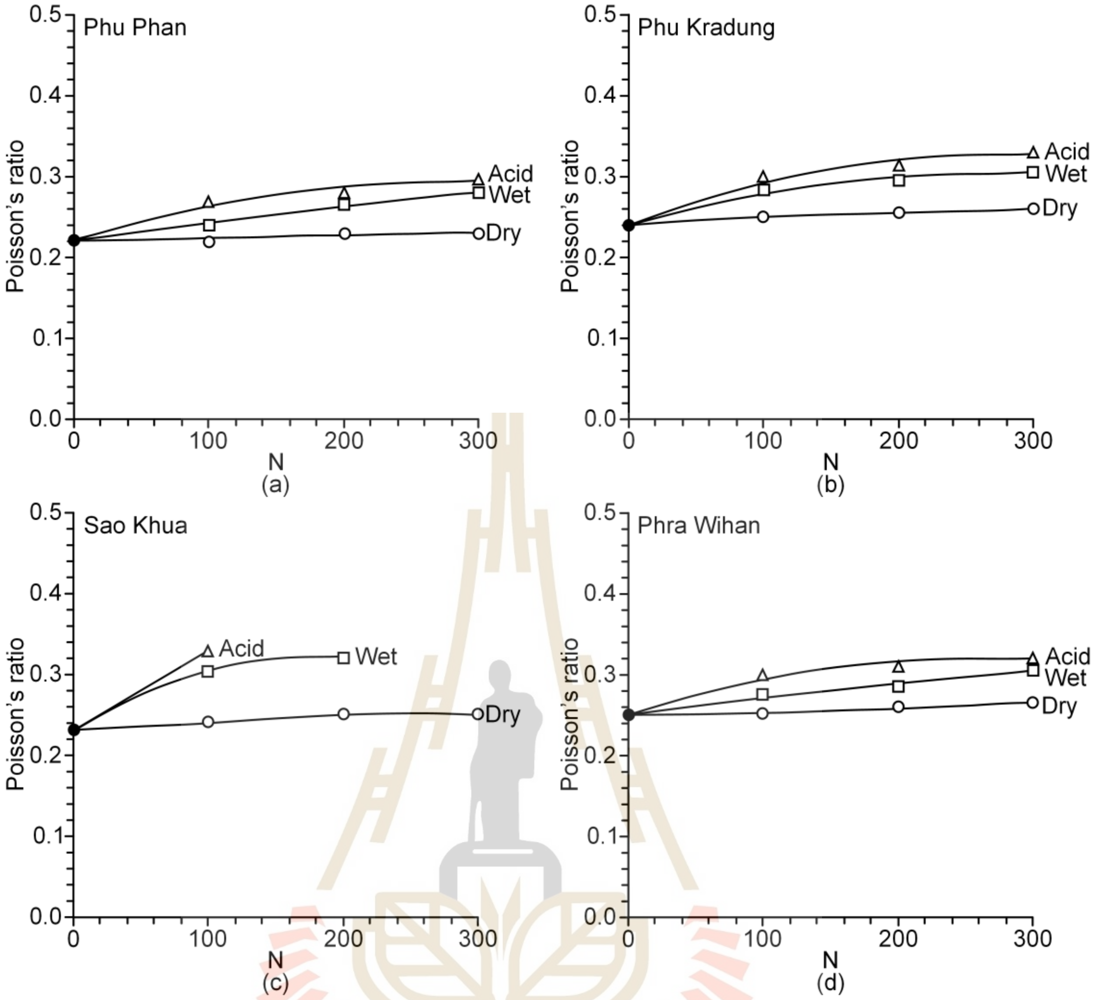

Figure 6.6 The relationship curve between Poisson's ratio and number of cycles (N) for Phu Phan (a), Phu Kradung (b), Sao Khua (c), and Phra Wihan (d) sandstones.

Table 6.6 Empirical constants for a polynomial relationship between ν and N.

Sandstone Type	Condition	$\nu_{(N)} = \alpha_\nu N^2 + \beta_\nu N + \nu_0$		Correlation Coefficients
		α_ν	β_ν	
Phu Phan	Dry	-3×10^{-8}	3×10^{-5}	0.7895
	Wet	-1×10^{-7}	0.0002	0.9944
	Acid	-9×10^{-7}	0.0005	0.9664
Phu Kradung	Dry	-1×10^{-7}	0.0001	0.9940
	Wet	-9×10^{-7}	0.0005	0.9739
	Acid	-1×10^{-6}	0.0006	0.9772
Sao Khua	Dry	-2×10^{-7}	0.0001	0.9809
	Wet	-3×10^{-6}	0.0010	1
	Acid	0	0.0010	1
Phra Wihan	Dry	1×10^{-7}	9×10^{-6}	0.9298
	Wet	-2×10^{-7}	0.0002	0.9790
	Acid	-1×10^{-6}	0.0005	0.9710

Notes: α_ν and β_ν are empirical constants

N is number of test cycle

ν_0 represents the Poisson's ratio at initial conditions

CHAPTER VII

DISCUSSIONS, CONCLUSIONS AND RECOMMENDATIONS FOR FUTURE STUDIES

7.1 Discussions

It is recognized that the sandstone formations from which the specimens are obtained show significant variations in terms of their mineral compositions from varying locations (DMR 2001; Racey et al., 1996). The mineral compositions of the test specimens determined here however can be useful to understand or compare the sandstone properties and durability under different environments.

The thermal and wetting-drying effects shown in this study may not be strictly true for other sandstone types and in particular for other rock type (e.g. granites, marble, shales, etc.). Other sandstones that have significantly different compositions and texture from those tested has may exhibit different behavior of degradations when subjecting to thermal and wetting-drying cycles.

The equivalent quartz content proposed here to reveal the effect of weathering on the changes of mineral compositions of the sandstones may not be applicable to other rock types where their minerals composing rocks have similar strengths and durability. As a result, different approaches may be required to access the weathering effect on the rock mineral compositions.

Admittedly the number of test specimens used here tend to be limited: one for each sandstone type and cooling condition. This is primarily due to the limited oven space and project duration (10 months). The test results, nevertheless, tend to show clear trends of rock deterioration in the forms of the reduction of physical and mechanical properties. The designed test cycles are aimed at accelerating and enhancing the weathering process, and hence reveals the long-term responses of the test sandstones in terms of density, strength, elastic modulus and mineral compositions.

Correlation between the test duration (300 days) with those of the actual duration under in-situ condition may not be possible at this time. This is due to the fact that the sandstone specimens are subjected to the temperature up to 105 °C (during 12 hrs. of heating) and immediately (2-3 minutes) cooled by submerging in the water or acid. This temperature is significantly higher than those occur naturally in southeast Asia. It is postulated that the rapid cooling by submerging in liquid may induce micro-cracks in the rock matrix. These cracks can propagate deeper and eventually becomes preferential flow paths allowing the liquid, particularly acid, to further dissolve the other mineral. This could explain why the rock density becomes lower as the test cycles increase. The increase of the sandstone porosity and micro-cracks with the test cycles cause the decrease of strength and stiffness of the sandstones. Under dry condition, all sandstones tend to be insensitive to heating (up to 105 °C) and slow cooling under ambient temperature. The results obtained here agree reasonably with those of Deng et al., (2012), Özbek (2014), Hua et al. (2015), Khanlari and Abdilor (2015), Liu et al., (2016), Zhao et al., (2017), Zhou et al. (2017)

and Sun and Zhang (2019) who investigate the physical and mechanical properties of sandstones under wetting and drying cycles.

Correlations between the test conditions used in the laboratory with those of the actual conditions are extremely difficult, if not impossible. The weathering processes are the coupled effects of thermo-mechanical and thermo-chemical processes. It is true that accurate prediction of the rock physical and mechanical properties under long-term weathering may be useful to for conservation and renovation of ancient monuments. Such effort may however requires undesirable destructive materials, e.g. hardness and strength testing.

7.2 Conclusions

Results from this study can be used for the selection criteria of sandstone type and the application of these sandstones under appropriate environments and locations. The conclusions from our study can be drawn as follows:

- All sandstones tend to be durable under dry condition even they are cyclically subjected to heating up to 105 °C for 300 cycles.
- Water and particularly acid can cause significant increase of sandstone porosity, and hence reduces their density. Sao Khua sandstone is highly sensitive to liquids, compared to the other three sandstones.
- Micro-cracks induced by heating and relatively rapid cooling can propagate deeper in to the rock matrix as the test cycles increase. They become preferential paths allowing the liquid to penetrate farther.
- As evidenced by the increase of equivalent quartz content, the sandstones lose more other minerals than quartz gains as the test cycles increase.

Another mineral durable less than quartz can be dissolved more easily than quartz grains.

- The loss of mineral compositions means that the sandstones lose cohesive bonding which leads to the reductions of compressive and tensile strengths and of the compressive and tensile elastic moduli. When the rocks become more porous, they can laterally dilate more under axial loading, and hence their Poisson's ratio increases with the test cycles.

7.3 Recommendations for future studies

The limitation of number and type of specimens of the research investigation and results discussed above lead to the recommendations for further studies, as follows.

1. Larger specimen numbers and sizes may be used to enhance the representativeness of the test results.
2. A more diverse sandstone type, composition and texture are desirable in order to truly assess all factors affecting the rock degradation.
3. Longer test duration may be needed for durable sandstones to obtain a better mathematical representation of their properties as affected by the weathering simulation parameters.
4. Thermo-mechanical and chemical analyses on the wet-dry cyclic specimens may be needed to correlate the laboratory test result with actual in-situ conditions.

REFERENCES

Abramson, L.W., Lee, T.S., Sharma, S., and Boyce, G.M. (1995). **Slope Stability and Stabilization Methods.** New York: John Wiley & Sons.

Andreotti, S., Franzoni, E., Degli Esposti, M., and Fabbri, P. (2018). Poly (hydroxyalkanoate) s-based hydrophobic coatings for the protection of stone in cultural heritage. **Materials.** 11(1): 165-190.

Andrews, D.E., Withiam, J.L., Perry, E.F., and Crouse, H.L. (1980). **Environmental effects of slaking of surface mine spoils: eastern and central United States.** Final Report. Contract No. J0285024. Bureau of Mines, United State Department of the Interior, Denver, United States of America.

ASTM C127-15 (2015). **Standard test method for determination of the specific gravity and water absorption of coarse aggregate**. Annual book of ASTM standards, American Society for Testing and Materials, West Conshohocken, PA.

ASTM C293/C293M-16 (2016). **Standard test method for flexural strength of concrete (Using simple beam with center-point loading)**. Annual book of ASTM standards, American Society for Testing and Materials, West Conshohocken, PA.

ASTM D7012-14e1 (2014). **Standard test methods for compressive strength and elastic moduli of intact rock core specimens under varying states of stress and temperatures.** Annual book of ASTM standards, American Society for Testing and Materials, West Conshohocken, PA.

Barbour, T.G., Atkinson, R.H., and Ko, H.Y. (1979). Relationship of mechanical, index and mineralogical properties of coal measure rock. **Twentieth Symposium on Rock Mechanics.** Austin, Texas. pp. 189-198.

Barzoi, S. C. and Luca, A. C. (2013). Significance of studying the petrography and mineralogy of the geological environment of old rupestrian churches to prevent their deterioration. A case study from the South Carpathians. **Journal of Cultural Heritage.** 14(2): 163-168.

Bell, F.G. (1978). The physical and mechanical properties of the fell sandstones, Northumberland, England. **Engineering Geology.** 12(1): 1-29.

Brace, W. F. (1961). Dependence of fracture strength of rocks on grain size. In **Proceedings of the 4th United States Rock Mechanics Symposium.** (pp. 99-103). University Park, Penn.

Charola, A.E. (1987). Acid rain effects on stone monuments. **Journal of Chemical Education.** 64(5): 436.

Deng, H. F., Li, J. L., Zhu, M., Wang, K. W., Wang, L. H., and Deng, C. J. (2012). Experimental research on strength deterioration rules of sandstone under "saturation-air dry" circulation function. **Rock and Soil Mechanics**. 33(11): 3306-3312.

Department of Mineral Resources. (2001). **Geology of Thailand**. Department of Mineral Resources, Ministry of Industry, Bangkok, Thailand (in Thai).

Fahy, M.P. and Guccione, M.J. (1979). Estimating strength of sandstone using petrographic thin-section data. **Engineering Geology.** 16(4): 467-485.

Franklin, B. J., Young, J. F., and Powell, R. (2014). Testing of Sydney dimension sandstone for use in the conservation of heritage buildings. **Australian Journal of Earth Sciences.** 61(3): 351-362.

Fuenkajorn, K. and Sri-In, T. (2009). Prediction of long-term strength of some weak rocks. **Engineering Journal of Research and Development.** 20(4): 1-12.

Ghobadi, M.H. and Momeni, A.A. (2011). Assessment of granitic rocks degradability susceptive to acid solutions in urban area. **Environmental Earth Sciences.** 64(3): 753-760.

Gökceoğlu, C., Ulusay, R., and Sönmez, H. (2000). Factors affecting the durability of selected weak and clay-bearing rocks from Turkey, with particular emphasis on the influence of the number of drying and wetting cycles. **Engineering Geology.** 57(3-4): 215-237.

Gunsallus, K.T. and Kulhawy, F.H. (1984). A comparative evaluation of rock strength measures. **International Journal of Rock Mechanics and Mining Sciences and Geomechanics Abstracts.** 21(5): 233-248.

Gupta, V. and Ahmed, I. (2007). The effect of pH of water and mineralogical properties on the slake durability (degradability) of different rocks from the Lesser Himalaya, India. **Engineering Geology.** 95(3-4): 79-87.

Hale, P. A. and Shakoor, A. (2003). A laboratory investigation of the effects of cyclic heating and cooling, wetting and drying, and freezing and thawing on the compressive strength of selected sandstones. **Environmental and Engineering Geoscience.** 9(2): 117-130.

Handlin, J. and Hager, R.V. (1957). Experimental deformation of sedimentary rock under a confining pressure. **Journal American Association of Petroleum Geologists.** 41: 1-50.

Hoek, E. (1965). **Rock Fracture Under Static Stress Conditions.** Mechanical Engineering Research Institute. Report MEG383, Council for Scientific and Industrial Research. South Africa.

Hua, W., Dong, S., Li, Y., Xu, J., and Wang, Q. (2015). The influence of cyclic wetting and drying on the fracture toughness of sandstone. **International Journal of Rock Mechanics and Mining Sciences.** 100(78): 331-335.

Khanlari, G. and Abdilor, Y. (2015). Influence of wet-dry, freeze-thaw, and heat-cool cycles on the physical and mechanical properties of Upper Red sandstones in central Iran. **Bulletin of Engineering Geology and the Environment.** 74(4): 1287-1300.

Kolay, E. and Kayabali, K. (2006). Investigation of the effect of aggregate shape and surface roughness on the slake durability index using the fractal dimension approach. **Engineering Geology.** 86(4): 271-284.

Lee, S. (2016). **The Third Periodic Report on the State of Acid Deposition in East Asia, Part II National Assessments.** Report No. ISSN 2432-8316. Acid deposition monitoring network in east Asia, Niigata-shi, Japan.

Lin, M. L., Jeng, F. S., Tsai, L. S., and Huang, T. H. (2005). Wetting weakening of tertiary sandstones-microscopic mechanism. **Environmental Geology.** 48(2): 265-275.

Liu, X., Wang, Z., Fu, Y., Yuan, W., and Miao, L. (2016). Macro/micro testing and damage and degradation of sandstones under dry-wet cycles. **Advances in Materials Science and Engineering.** 2016 (1): 1–16.

Moon, V. and Jayawardane, J. (2004). Geomechanical and geochemical changes during early stages of weathering of Karamu basalt, New Zealand. **Engineering Geology.** 74(1): 57-72.

Moradizadeh, M., Cheshomi, A., Ghafoori, M., & Tarigh Azali, S. (2016). Correlation of equivalent quartz content Slake durability index and Is_{50} with Cerchar abrasiveness index for different types of rock. **International Journal of Rock Mechanics and Mining Sciences.** 86: 42-47.

Nahon D.B. (1991). **Introduction to the Petrology of Soils and Chemical Weathering.** John Wiley and Sons. New York.

Ning, L., Yunming, Z., Bo, S., and Gunter, S. (2003). A chemical damage model of sandstone in acid solution. **International Journal of Rock Mechanics and Mining Sciences.** 40(2): 243-249.

Özbek, A. (2014). Investigation of the effects of wetting-drying and freezing-thawing cycles on some physical and mechanical properties of selected ignimbrites. **Bulletin of Engineering Geology and the Environment.** 73(2): 595-609.

Pardini, G., Guidi, G. V., Pini, R., Regüés, D., and Gallart, F. (1996). Structure and porosity of smectitic mudrocks as affected by experimental wetting-drying cycles and freezing-thawing cycles. **Catena.** 27(3-4): 149-165.

Racey, A., Love, M. A., Canham, A. C., Goodall, J. G. S., Polachan, S., and Jones, P. D. (1996). Stratigraphy and reservoir potential of the Mesozoic Khorat Group, NE Thailand: Part 1: stratigraphy and sedimentary evolution. **Journal of Petroleum Geology.** 19(1): 5-39.

Robinson, D.A. and Williams, R.B.G. (1994). **Rock Weathering and Landform Evolution.** John Wiley and Sons. New York.

Shakoor, A. and Bonelli, R.E. (1991). Relationship between petrographic characteristics, engineering index properties and mechanical properties of selected sandstones. **Bulletin of the Association of Engineering Geologists.** 28(1): 55-71.

Siedel, H., Neumeister, K., and Sobott, R. J. G. (2003). Laser cleaning as a part of the restoration process: Removal of aged oil paints from a Renaissance sandstone portal in Dresden, Germany. **Journal of Cultural Heritage.** 4: 11-16.

Sri-in, T. and Fuenkajorn, K. (2007). Slake durability index strength testing of some weak rocks in Thailand. In **Proceedings of the 1st Thailand Symposium on Rock Mechanics.** (pp. 145-159). Nakhon Ratchasima.

Sumner, P. D., and Loubser, M. J. (2008). Experimental sandstone weathering using different wetting and drying moisture amplitudes. **Earth Surface Processes and Landforms: Journal of the British Geomorphological Research Group.** 33(6): 985-990.

Sun, Q., and Zhang, Y. (2019). Combined effects of salt, cyclic wetting and drying cycles on the physical and mechanical properties of sandstone. **Engineering geology.** 248: 70-79.

Torres-Suarez, M. C., Alarcon-Guzman, A., and Berdugo-De Moya, R. (2014). Effects of loading–unloading and wetting–drying cycles on geomechanical behaviors of mudrocks in the Colombian Andes. **Journal of Rock Mechanics and Geotechnical Engineering.** 6(3): 257-268.

Tugrul, A. (2004). The effect of weathering on pore geometry and compressive strength of selected rock types from Turkey. **Engineering Geology.** 75(3-4): 215-227.

Tugrul, A. and Zarif, I. H. (1999). Correlation of mineralogical and textural characteristics with engineering properties of selected granitic rocks from Turkey. **Engineering Geology.** 51(4): 303-317.

Ulusay, R., Tureli, K., and Ider, M.H. (1994). Prediction of engineering properties of a selected litharenite sandstone from its petrographic characteristics using correlation and multivariate statistical techniques. **Engineering Geology.** 38(1-2): 135-157.

Xu, H. B., Tsukuda, M., Takahara, Y., Sato, T., Gu, J. D., and Katayama, Y. (2018). Lithoautotrophical oxidation of elemental sulfur by fungi including Fusarium solani isolated from sandstone Angkor temples. **International Biodeterioration & Biodegradation.** 126: 95-102.

Yokota, S. and Iwamatsu, A. (1999). Weathering distribution in a steep slope of soft pyroclastic rock as an indicator of slope instability. **Engineering Geology.** 55(1-2): 57-68.

Yusof, N. Q. A. M. and Zabidi, H. (2016). Correlation of mineralogical and textural characteristics with engineering properties of granitic rock from Hulu Langat, Selangor. **Procedia Chemistry.** 19: 975-980.

Zhang, B. Y., Zhang, J. H., and Sun, G. L. (2015). Deformation and shear strength of rockfill materials composed of soft siltstones subjected to stress, cyclical drying/wetting and temperature variations. **Engineering Geology.** 190: 87-97.

Zhao, Z., Yang, J., Zhang, D., and Peng, H. (2017). Effects of wetting and cyclic wetting–drying on tensile strength of sandstone with a low clay mineral content. **Rock Mechanics and Rock Engineering.** 50(2): 485-491.

Zhou, Z., Cai, X., Chen, L., Cao, W., Zhao, Y., and Xiong, C. (2017). Influence of cyclic wetting and drying on physical and dynamic compressive properties of sandstone. **Engineering geology.** 220: 1-12.

BIOGRAPHY

Miss Pratabjai Prasujan was born on October 31, 1995 in Ubon Ratchathani Province, Thailand. She received her Bachelor's Degree in Engineering (Geotechnology) from Suranaree University of Technology in 2018. For her post-graduate, she continued to study with a Master's degree in Civil, Transportation and Geo-resources Engineering Program, Institute of Engineering, Suranaree University of Technology. During graduation, 2018-2020, she was a part time worker in position of research assistant at the Geomechanics Research Unit, Institute of Engineering, Suranaree University of Technology.